Lithium-rich geothermal brines in Europe: An up-date about geochemical characteristics and implications for potential Li resources

Bernard Sanjuan Sanjuan, Blandine Gourcerol, Romain Millot, Detlev Rettenmaier, Elodie Jeandel, Aurélien Rombaut

Lithium-rich geothermal brines in Europe: an up-date about geochemical characteristics and implications for potential Li resources

Bernard Sanjuan[1], Blandine Gourcerol[1], Romain Millot[1], Detlev Rettenmaier[2], Elodie Jeandel[2], Aurélien Rombaut[3]

[1]BRGM, F-45060, Orléans, France

[2]EIFER, D-76131, Karlsruhe, Germany

[3]ERAMET Marketing Services, F-75015, Paris, France

Abstract

Lithium (Li) is a strategic metal - especially for batteries in electric vehicles - for which worldwide demand is constantly increasing. Presently, several investigations are examining if a part of lithium could be extracted from deep European geothermal fluids. Among the data from geothermal and hydrocarbon wells found in the literature review carried out by BRGM and EIFER, only six areas stand out with deep fluids containing high Li concentrations from 125 to 480 mg/l in Italy, Germany, France and the United-Kingdom. Except the UK fluid, which has a relatively low salinity (TDS = 19 g/l) and reservoir temperature (around 52 °C) as well as the lowest Li concentration (125 mg/l), these deep Li-rich fluids are Na-Cl brines (TDS ≥ 56 g/l) with high concentrations of Na (> 18 g/l) and Cl (> 25 g/l) and high temperatures (≥ 120 °C and up to 380 °C in Italy). If high TDS and temperature values seem to be key factors for triggering high Li concentrations in such fluids, these two factors alone cannot be sufficient. Indeed, our study

confirms that Li concentrations not only depend on temperature and fluid salinity, but also on the type of reservoir rock and its mineralogical constituents, as demonstrated by the good results obtained using two different Na-Li thermometric relationships existing in the literature. One fits well with the brines from low to high temperature (120-250 °C) reservoirs in deep tectonic sedimentary basins over a crystalline basement (France, Germany) and the other with the fluids from ultra-high temperature (≥ 300 °C) reservoirs in volcano-sedimentary environment (Italy). If the high chloride concentrations values in these brines mainly depend on the fluid origin (evaporated seawater or freshwater, halite dissolution, primary neutralization fluids or parent-geothermal fluids in high-temperature and -pressure volcanic environments, water mixing, etc.), the other aqueous major species are mostly controlled by hydrothermal water-rock interaction processes. At these temperatures (≥ 120 °C), the fluid-rock interaction processes are generally dominated by plagioclase and K-feldspar dissolution, followed by albitization of these minerals, dissolution of white micas and biotite, precipitation of illite, and chloritization. According to the two Na-Li thermometric relationships, existing mineralogical and isotopic data, this study suggests that the main sources of Li are white micas and biotite dissolution. Among the European areas, it shows that the Upper Rhine Graben (URG) along the French/German border is probably the most promising zone. For the URG geothermal brines, the main source and control of lithium, at about 225 °C, at reservoir depth, is probably the up to 450-m-thick micaceous continental sandstone of Triassic Buntsandstein. A minor contribution from the granite basement can also not be excluded. Though the Li concentration values of these brines (≥ 150 mg/l) seem to be favourable for geothermal Li exploitation, it is essential to make an as accurate as possible estimate of the Li resource of these brines, design the Li extraction process, and examine the economic conditions of its exploitation.

Key words: lithium, temperature, Rhine Graben, micas, sandstone, granite

1. Introduction

Lithium (Li) and its chemical compounds are widely used in numerous industries such as glass, ceramics, lubricating grease, or polymer production. With the recent development of electro-mobility and the evolution of energy systems to achieve Green Deal goals, energy storage devices and batteries are significant new market segments for lithium, thus driving an increasing demand for this metal. In 2008, global lithium consumption was 21,300 t of Li metal, with 20% for (rechargeable) batteries (4,260 t of Li metal), whereas in 2019, total consumption had more than doubled to about 48,500 t Li, with 54% or 26,190 t Li metal for rechargeable batteries (Gourcerol *et al.*, 2021). Consequently, many mining companies, governments and private investors seek to supply this continuously increasing demand with new mine openings as well as expanding producing mines, and encouraging projects for Li-ion battery recycling.

Li is widely distributed on the Earth, with concentrations of 24 ppm in the upper continental crust, 12 ppm in the middle continental crust, 13 ppm in the lower continental crust, and 1.5 ppm in the mantle (Jagoutz *et al.*, 1979; Rudnick and Gao, 2014; Liu *et al.*, 2018). The mean Li concentration in seawater is 0.18 mg/l (Riley and Tongudai, 1964). In most rocks, silicate minerals, especially Mg-rich silicates, are the almost exclusive hosts for Li (Misra and Froelich, 2012) because Li can have a similar radius to Mg (Shannon, 1976), depending on its coordination number in these minerals. High Li contents can be identified in intermediate-acid rock bodies, in igneous rocks (granite, pegmatite; Li *et al.*, 2018a), in volcanic tuff and rhyolite (Li *et al.*, 2018b), and in detrital materials (e.g., lacustrine deposits, sandstone).

Lithium resources are historically divided into three types: 1) hard-rock deposits, 2) surface and near surface brines, and 3) unconventional resources such as seawater or deep geothermal brines. Hard-rock deposits reflect endogenous/exogenous processes and may be related to magmatic and sedimentary rocks (Kesler *et al.*, 2012; Gourcerol *et al.*, 2019). Li-bearing minerals are numerous (spodumene, petalite, lepidolite, hectorite, jadarite, etc.) and require various processes for extracting lithium. Surface brines refer to arid to semi-arid salt pans and

ephemeral salt lakes in tectonically active sedimentary basins, called "*salars*" in South America. Extracting lithium from these salt lakes is relatively easy and cheap, compared to the complex and energy-intensive extraction technologies involved for hard-rock deposits, which may require several chemical transformations. The most known salt pans are located in the lithium triangle - also called lithium ABC (Argentina, Bolivia, Chile) - which stretches from northern Argentina (*salar* de Hombre Muerto) to western Bolivia (*salar* de Uyuni) and northern Chile (*salar* de Atacama) and have been studied by numerous authors (Risacher, 1984; Risacher and Fritz, 2000; Risacher *et al.*, 2003; Kesler *et al.*, 2012; Godfrey *et al.*, 2013; Munk *et al.*, 2018; Schmidt, 2019; Garcia *et al.*, 2021; Lopez Steinmetz, 2021). High lithium contents can be found in these *salars* (up to 6,400 mg/l, being the maximum known Li concentration; Lopez Steinmetz *et al.*, 2018). Other well-known lithium-rich surface brines are found in the Qaidam Basin and on the Tibet plateau, in China (Li *et al.*, 2018a; 2019).

The near surface brines that are pumped from beneath the Clayton Valley in the Basin and Range extensional province of Nevada, USA, from depths of about 100-250 m, into evaporating ponds (Barrett and O'Neil, 1970; Davis *et al.*, 1986; Ventura *et al.*, 2016) have produced lithium-metal since the mid-1960s and are the only producer in North America. Such brines contain about 20% NaCl and up to 400 ppm of lithium. Their formation was studied in detail by Davis *et al.* (1986).

Our present work only deals with unconventional European Li resources, such as deep geothermal and oil & gas field Li-rich brines, which were identified to assess the lithium resources that could be extracted from these brines for supplying Europe with this metal. Outside Europe, Li-rich deep brines (up to 983 mg/l of Li) are found in some geothermal fields like Salton Sea, in California, USA (Werner, 1970; Elders and Cohen, 1983; Williams and McKibben, 1989; Sanjuan and Millot, 2009), in the Siberian sedimentary platform (Shouakar-Stash *et al.*, 2007; Alekseeva and Alekseev, 2018), or in the Tibet Plateau (Li *et al.*, 2018a; 2019). Average Li contents of oilfield brines are usually below 10 mg/l, but brines with high Li

concentrations of up to 500 mg/l occur in some hydrocarbon source rocks (Blake, 1974; Collins, 1975; Connolly *et al.*, 1990; Moldovanyi *et al.*, 1993; Stueber *et al.*, 1993; Wilson and Long, 1993; Chan *et al.*, 2002; Williams and Hervig, 2005; Tabarès, 2013). High Li concentrations have also been observed in deep ocean thermal vents (Garrett, 2004).

Based on a state-of-the-art literature review and use of the BRGM-EIFER database for deep geothermal and oil-field Li-rich brines in Europe (Sanjuan *et al.*, 2019; 2020), here we present and discuss the main chemical and isotope characteristics of these brines. We also contribute to identify the main Li source in such deep brines, which is poorly known, and to understand natural processes of lithium enrichment, as the influence of temperature, fluid salinity and nature of the reservoir rocks. The resolution of such scientific questions is very important to launch and optimize the Li exploitation from geothermal brines.

2. Main Li-rich deep geothermal brines in Europe

In principle high-lithium concentrations (≥ 150 mg/l) are recommended for an economically effective Li extraction (Sanjuan *et al.*, 2020). Among the data of the BRGM-EIFER database, only six geothermal areas with deep fluids containing Li concentrations ranging from 125 to 480 mg/l are registered in Europe (Fig. 1), in Italy, Germany, France and the United Kingdom.

2.1 Main play types of geothermal systems

These areas, which were selected for this study, can be divided in two main play types of geothermal systems, as recommended by Sanyal (2005) and Moeck (2014):

- *ultra-high temperature geothermal systems* (≥ 300 °C), with Li concentrations ranging from 250 to 480 mg/l, in Mesozoic sedimentary reservoirs associated with relatively young volcanic environments (Quaternary volcanism), where the heat is provided by intrusive magmatic activity (presence of volcanic rocks and magma degassing), as the

two well-known geothermal areas in Italy: Cesano (Monte Sabatini area) in the Latium region, and Campi Flegrei in the Campania region (Calamai *et al.*, 1976; Carella and Guglielminetti, 1983; Pauwels *et al.*, 1991; Buonasorte *et al.*, 1993; Cinti *et al.*, 2011, 2017).

- *The Monte Sabatini area*

This area is located along the peri-Tyrrhenian sector of Central Italy. In this region, a post-collisional tectonic activity occurred during the Neogene, generating dominantly extensional NNW-SSE-trending fault systems and minor NE-SW-trending transtensive structures that accommodated differential extension. The progressive eastward migration of the extension wave produced a strong crustal thinning (> 25 km), high heat flow (locally > 200 mW/m^2) and subduction-related magmatism. Volcanic complexes grew up on buried horst-graben structures, whilst marine clastic sediments filled up the structure lows (Barberi *et al.*, 1994; Cinti *et al.*, 2017). This area was volcanically active from 0.60 to 0.08 Ma. The alkaline volcanic products overlay a tectono-stratigraphic sequence consisting of 1) a Plio-Pleistocene complex, consisting of conglomerates, sandstones and clays, 2) Cretaceous-Oligocene Ligurian and sub-Ligurian units, including calcareous-pelitic calcarenites and arenaceous-pelitic turbidites, 3) Mesozoic carbonates, and 4) Triassic evaporites (Burano Formation). In this region, mantle degassing and thermo-metamorphic processes feed a regional pressurized CO_2 gas system. The hydrogeological setting is dominated by a regional hydrothermal reservoir hosted in the Mesozoic carbonate-evaporite units.

- *The Campi Flegrei area*

This area is a large volcano situated to the west of Naples and was the result of voluminous Pliocene-Quaternary volcanism in the Campania margin, which presents peculiar physiographic, volcanic, and tectonic features and is of critical importance in understanding the tectonic and geodynamic evolution of the Tyrrhenian Sea back-arc

basin. Two alternative geodynamic models have been used to explain the evolution of the Tyrrhenian Sea-Apennine system. The subduction model maintains that subduction of the Adriatic-Ionian lithosphere and its slab retreat are responsible for an asymmetric migration of the extension in the Tyrrhenian upper plate. Instead, the astenosphere upwelling model invokes a lithospheric stretching driven by mantle astenosphere expansion due to the growth of a plume head (Torrente and Milia, 2015). The recent volcanism developed in the Campania tectonic depression formed at the borders of the Apennine mountain chain. Significant subsidence occurred in this depression, and the carbonate basement down-lifted by more than 3500 m below sea level. The presence of a shallow magmatic chamber of large dimensions provides the heat source for the geothermal system.

Both Italian geothermal areas in the Latium and Campania regions are high-pressure water dominated geothermal plays, and both present ultra-high temperatures (up to 380 °C). However, considering the high cost and other risks associated with their potential exploitation, both areas were abandoned a long time ago. In addition, high temperatures (≥ 340 °C), associated with hydrothermal and thermo-metasomatic phenomena, were measured in wells at depths of 2000-3000 m. These phenomena, implying large volumes of hot dry rock, often cause a drastic reduction in permeability that remains low if natural fracturing is not continually reactivated. Another negative factor for a cost-effective exploitation was the type of geothermal fluids, which were highly reactive, prone to scaling and with high concentrations of CO_2 and H_2S gases.

- *low to high temperature geothermal systems (120-250 °C)* without an associated magmatic heat source, with Li concentrations ranging from 140 to 210 mg/l, in deep tectonic sedimentary basins over a crystalline basement, which are less common and deeper (Nicholson, 1993), as the two German geothermal areas (Groβ Schönebeck geothermal site located in the North German Basin, about 50 km north of Berlin, and

South German Molasse Basin located in southwestern Germany), explicitly described by Regenspurg *et al.* (2010; 2015) and Stober (2014) respectively, and the Upper Rhine Graben (URG) area in both Germany and France (Fig. 2), where numerous Na-Cl brines discharged from deep wells have very similar features (Sanjuan *et al.*, 2016a; 2021; Bosia *et al.*, 2021).

- *The North German Basin*

The North German Basin is a passive-active rift basin located in central and west Europe, lying within the southeasternmost portions of the North Sea and the southwestern Baltic Sea and across terrestrial portions of northern Germany, Netherlands, and Poland. The North German Basin is a sub-basin of the Southern Permian Basin, that accounts for a composite of intracontinental rift basin composed of Permian to Cenozoic sediments, which have accumulated to thicknesses around 10-12 kilometres. The complex evolution of the basin takes place from the Permian to the Cenozoic, and is largely influenced by multiple stages of rifting, subsidence, and salt tectonic events.

- *The Molasse Basin*

The so-called Molasse Basin is a foreland basin of the Alps that formed during the Cenozoic Oligocene and Miocene because of the flexure of the European plate under the weight of the orogenic wedge of the Alps. The basin filled with a sedimentary sequence for the most part removed from the developing mountain chain by erosion and denudation. After several periods of tectonic subsidence and uplift in the alpine foreland, the Molasse Basin ceased to be an area of net sedimentation during the late Miocene and early Pliocene. The basis of the Molasse sedimentary units is formed by the Upper Jurassic and the Triassic series. The Upper Jurassic (Malm) limestone and the Middle Triassic Muschelkalk limestone are the major thermal aquifers in the Southwest German alpine foreland. The hydrochemical properties of the two aquifers differ in several

aspects. The total amounts of dissolved salts (TDS) are much higher within the Upper Muschelkalk aquifer than within the Upper Jurassic. With increasing depth, the total of dissolved salts increases. In the case of the Upper Muschelkalk, the fluid salinity is linked to deep circulation systems (Stober, 2014). The high Li concentrations (143-162 mg/l) observed in some deep wells (HC-14, HC-15 and HC-19) are rather limited to the Upper Muschelkalk aquifer and are not representative of the Molasse Basin geothermal fluids in general. The Li concentrations are much less in the Upper Jurassic aquifer (Stober, 2014). According to the temperature assessment given by the Na-K, Na-K-Ca and K-Mg geothermometers, the temperature of the brines discharged from the HC-14, HC-15 and HC-19 deep wells could be rather close to 190-200°C in the reservoir.

- *The Upper Rhine Graben (URG)*

The NNE-trending URG of the European Cenozoic Rift System (ECRIS) developed from ca. 47 Ma onwards in response to changing lithospheric stresses in the north-western foreland of the Alps (Grimmer *et al.*, 2017). The Graben itself, with an average width of 35 km and extending approximately 300 km from Frankfurt (Germany) in the north to Basel (Switzerland) in the south, is located in the upper-middle Rhine river basin (Fig. 3). It forms an evaporite setting mainly consisted of fine-grained, low energy silt-clay-marls with minor intercalations of sand, carbonates, and minor evaporites, in which the rifting process played a major role by a) providing the physical space for sedimentation, b) creating a series of intermediate basins, and c) facilitating a network of faults along the active rift margins that promoted fluid circulation and controlled water exchanges with other basins and/or the open sea. The Graben's Palaeozoic crystalline basement, underlying a Mesozoic to Cenozoic sedimentary cover as much as 4-5 km thick in its asymmetrical centre (Fig. 4), comprises massive granite (334 ± 3.8 Myr; Cocherie *et al.*, 2004), the top of which, where unaltered, is a porphyritic granite with quartz, K-feldspar megacrysts, plagioclase, biotite, hornblende and accessory titanite, apatite, zircon and

magnetite. However, the crystalline basement of the URG does not consist solely of granites: in the Baden-Baden 1, quartz-phyllites were drilled and in the west of Wissembourg, a basement outcrop exposes steep dipping meta-greywacke and volcanic rocks. The low-metamorphic rocks of the Baden-Baden zone and the northern Vosges trend NE-SW across the URG are therefore expected to occur in the subsurface, likely intruded by granites, but it is highly unlikely to expect that there is nothing else but granite. In the Kaiserstuhl volcanic rocks, xenoliths comprise amphibolites and gneisses documenting that the crystalline basement contains rocks different from granite (Wimmenauer, 2003). The overlying sedimentary sequences, which are relatively well known from several oil- and mineral-exploration studies and from the drilling of numerous oil wells (Le Masne and Lambert, 1993), consist of Cenozoic evaporites and claystone underlain by Mesozoic limestone and sandstone. Cenozoic evaporites comprise major portions of the stratigraphic succession in the southern Graben (Eocene - Oligocene Wittelsheim Fm) and in the northern URG (Corbicula beds of the Landau Fm), where halite layers occur (e.g. Worms area). Intervals of relatively high permeability within the sedimentary succession make up the major aquifers, of which the most important is the Triassic Buntsandstein red sandstone composed of continental conglomerate to siltstone with interbeds of claystone and dolomite (Aquilina et al., 1997; Duringer *et al.*, 2019). In this area, several geothermal sites have been developed with doublets drilled down to the granite basement in France (Soultz-sous-Forêts and Rittershoffen) and in Germany (Landau and Insheim). Another geothermal doublet in Germany (Bruchsal) has been drilled down to the lower Buntsandstein and the top of Permian (Bertleff *et al.*, 1988; Kölbel *et al.*, 2020). An old geothermal well was drilled down to this aquifer, at Cronenbourg, in France, in 1980 (Fig. 3). Several geothermal projects are ongoing, or under investigation (Vendenheim, Illkirch, in Alsace, France; Sanjuan *et al.*, 2021; Bosia *et al.*, 2021), for exploiting the hot fluids (≥ 160 °C) circulating in the deeper parts of the Basin and in the upper fractured part of the granite

basement, in order to produce electricity or/and heat. For the time being, these six geothermal sites are the only ones with wells drilled down to the URG granite basement, thus constituting the only direct source of information about the chemical and isotopic compositions of fluids circulating in this basement.

The South Crofty mine, in Cornwall, United Kingdom, where economic vein deposits of Sn, Cu, Pb and Zn of Variscan age were found in the Carnmenellis granite which forms a near-circular outcrop of the Cornubian batholith intruded about 290 Ma ago into Devonian argillaceous sedimentary rocks (Wheildon *et al.*, 1980; Edmunds *et al.*, 1985) can be considered as a very low temperature geothermal system (< 100°C), but the Li concentrations in the fluids (> 125 mg/l) are lower than in the previous geothermal systems. The last saline groundwaters (up to 19 g/l) are found in four tin mines in granite or its thermal aureole, as well as in several closed mines along the northern margin of the granite belt. They generally show discharges between 1 and 10 l/s, occur at depths between 200 and 700 m below surface and have discharge temperatures up to 52°C.

2.2 Quality and representativeness of the analytical data

The main geothermal and geological characteristics of the six European areas with deep Li rich-brines, as well as the chemical and isotope compositions of these brines, are reported in Table 1 and Table 2, respectively. No analytical data was produced during this study. All the data were selected from the literature review carried out during this study. The geochemical and physical data in the database are relatively heterogeneous, being well-documented and numerous for some geothermal sites, such as Soultz-sous-Forêts, Rittershoffen, Vendenheim, Illkirch, Insheim, Landau and Bruchsal, in the Upper Rhine Graben (URG), but rare and poorly-documented for other sites, especially for old data on the Cesano and Campi Flegrei sites in Italy. For comparison and discussion, the main characteristics of the Salton Sea geothermal area, located in the volcanic Imperial Valley, USA, well-known for its Li rich-brines, and the corresponding chemical compositions, have also been reported in these tables.

Except the old data from archives for the brine discharged from the Cronenbourg well in the URG (Pauwels *et al.*, 1993), and from the wells located in the two Italian geothermal areas (Pauwels *et al.*, 1991), in the Molasse Basin (Stober, 2014), and in the South Crofty in Cornwall (Edmunds *et al.*, 1985), the fluid sampling conditions, used analytical methods and associated uncertainty are given for all the other geothermal brines by the corresponding authors. So, for example, in May 2013 and in February 2014, deep fluid samples were collected with a Leutert Positive Displacement Sampler (PDS) at *in situ* P-T conditions at different depths of the Groβ Schönebeck production well (Regenspurg *et al.*, 2015) and a detailed description of the fluid sampling procedure is given by Regenspurg *et al.* (2010). For the URG brines (Sanjuan *et al.*, 2016a; 2021; Bosia *et al.*, 2021), the geothermal brines were collected at the well-head during normal operating conditions of the existing power plants (Soultz, Rittershoffen, Insheim, Landau, Bruchsal) or during production tests, when there are only wells (Vendenheim, Illkirch). Even if the quality of the old data is difficult to assess, we estimate that most of the data, especially the major species and lithium, in high concentrations, can be considered as representative of the deep reservoir brines. In the URG, the numerous fluid samples collected at different depths between 3500 and 5000 m, at Soultz-sous-Forêts, have indicated that the chemical and isotopic compositions of all these brines was homogeneous (Sanjuan *et al.*, 2010). Moreover, similar fluid chemistry is observed for all the deep brines from the URG (Sanjuan *et al.*, 2016a; 2021; Bosia *et al.*, 2021). Comparable conclusions were performed by Regenspurg *et al.* (2015) for the brines collected at different great depths from the Groβ Schönebeck production well.

In contrast, the pH values measured at surface are indicative and must be calculated using geochemical modelling to have a representative value of the fluid in the reservoir conditions. As only the concentrations of sodium, potassium and lithium (under a logarithmic form) are used in this study for geothermometric and thermodynamic considerations, the uncertainty of the old

307 data, which could be higher than that usually observed (3-5% for major species and 10-15% for
308 trace species), should have minimal impact on these results.

309

310 3. Main chemical fluid characteristics

311 Figure 5, showing Cl *versus* Na concentrations and Li-concentration levels, indicates that the
312 deep Li-rich fluids found in the BRGM-EIFER database (Li ≥ 90 mg/l) are generally Na-Cl brines
313 with high concentrations of dissolved Na (> 18 g/l) and Cl (> 25 g/l), and TDS values over 56 g/l.
314 As indicated in Table 1, all deep European Li-rich brines also have reservoir temperatures
315 above 120 °C. Only the South Crofty mine fluids (UK) with lower salinity values (Na = 4.3 g/l, Cl
316 = 11.5 g/l; TDS = 19 g/l), have lower temperatures, close to 52 °C (Edmunds *et al.*, 1985).

317 Other European high-salinity fluids of the database, with high Na and Cl concentrations, but low
318 temperatures (Paris Basin, Landau oilfields and North Sea oilfields, for example), have relatively
319 low Li concentrations (Fig. 5). Similarly, high-temperature geothermal fluids (≥ 250 °C) in
320 worldwide volcanic environments (El Tatio in Chile, Wairakei in New Zealand, Bouillante in
321 Guadeloupe, or Reykjanes in Iceland; Sanjuan and Millot, 2009), which have moderate salinity
322 values ranging from 10 to 40 g/l, indicate relatively low Li concentrations (2 to 35 mg/l).

323 After Munk *et al.* (2018), the geochemical processes that can explain the evolution of inflow
324 waters to brine formation in the basins include evaporation processes, low-temperature
325 weathering, formation of transition zone brines, and halite precipitation-dissolution cycles. The
326 lithium in the deep Li-rich brines therefore results from a complex history, which needs the
327 formation of preliminary Na-Cl brines formed by different processes depending on the geological
328 environment.

329 Deep Li-rich geothermal brines can have several origins:

330 - brines formed by seawater evaporation (up to halite - NaCl - precipitation, at least)
331 in closed catchment basins during dry and warm periods, with cycles of halite

precipitation-dissolution following successive marine transgression-regression periods and mixing with freshwaters, as described for most of the brines formed from the Triassic to the Oligocene in the URG (Sanjuan *et al.*, 2016a). Indeed, during the Mesozoic, after a period of continental siliciclastic fluvial sedimentation in the Buntsandstein (Lower Triassic), due to the erosion of the Hercynian massifs under a tropical climate, a great part of France was flooded by the sea in the Muschelkalk (Middle Triassic). In the east of France where is located the URG, this sea was named German or Muschelkalk Sea. Due to several level decreases of this shallow and warm sea, the Keuper (Upper Triassic) is shown to be the result of evaporitic brines and sedimentation under a tropical climate. In the Jurassic, the major part of France was again flooded by the sea and a big amount of marine sediments was deposited. The Upper Jurassic and the Lower Cretaceous are characterized by a marine regression followed by the big Cenomanian-Turonian marine transgression in the Upper Cretaceous. The sea again receded at the end of the Cretaceous. There are no Cretaceous sediments preserved in the subcrop of the URG due to late Cretaceous inversion and doming (e.g. Grimmer *et al.*, 2017). Doming was associated with intrusion and extrusion of minor low-percentage melt foidites and alkali-basalts, terminated at ca. 47 Ma when URG formation has started (e.g. Grimmer *et al.*, 2017). The URG was the object of several marine transgressions from North Sea or Tethys Ocean during the Oligocene, at the end of the Paleogene (first period of the Cenozoic), characterized by a tropical climate in France and the setting of the present URG. This area sometimes constituted a strait between the North Sea and the Tethys Ocean in the south. During the marine regressions, lagoons and lakes were formed and evaporite minerals (gypsum, halite, etc.) were deposited during the dry periods. For example, the halite and potash salts in South Alsace, in France, and in SW Germany, were deposited in the late Eocene - early Oligocene (Wittelsheim Fm). The Chattian, at the end of the

Oligocene, marks the end of the marine transgressions in the URG and continental facies replaced marine or evaporitic deposits;

- brines formed by freshwater evaporation and evaporite dissolution (e.g., Salton Sea geothermal reservoir, USA: Elders and Cohen, 1983; Mc Kibben *et al.*, 1987; Williams *et al.*, 1989; Lippmann *et al.*, 1999; Birkle *et al.*, 2010);
- primary neutralization or parent geothermal Na-Cl brines in high-temperature and -pressure volcanic environments associated with relatively recent magmatic activity (Giggenbach, 1992; Hedenquist, 1995);
- a combination of several of the aforementioned processes;
- brines formed by water-rock interaction processes, as in Cornwall, UK (Edmunds *et al.*, 1985).

For most of these brines, elements such as chloride and bromide are present in high concentrations and are commonly used for constraining the fluid origin, as well as the water stable isotopes δD and $\delta^{18}O$ (Rittenhouse, 1967; Fontes and Matray, 1993; Stober and Bucher, 1999a and b; Sanjuan *et al.*, 2016a; 2021). The chloride and bromide concentrations are high in seawater and during the deposition of halite due to seawater evaporation, the Cl/Br ratio decreases compared to that of seawater because Br is lowly incorporated in this mineral. Converserly, the fluids which dissolve halite, indicate higher Cl/Br ratios than that of seawater (Rittenhouse, 1967; Sanjuan *et al.*, 1990; Fontes and Matray, 1993). During the formation of sedimentary basins, surficial brines are buried with their geological formation or transferred to other, deeper, formations. The degree of water mineralization increases under the influence of increasing temperature (Lin *et al.*, 1996; 2001; 2002).

Except chloride, the major aqueous species of the deep brines are mostly controlled by hydrothermal water-rock interaction processes at medium and high temperatures (≥ 120 °C). Fluid-rock interaction is generally dominated by plagioclase and K-feldspar dissolution, followed

384 by albitization of these minerals, dissolution of white micas and biotite, and precipitation of illite
385 and chloritization (Sanjuan *et al.*, 2019). For instance, an increase of dissolved calcium and a
386 decrease of aqueous sodium can be observed with increasing temperature, due to plagioclase
387 dissolution and albite precipitation (op. cit.):

388 $$CaAl_2Si_2O_8 \text{ (anorthite)} + 4\ SiO_2 \text{ (quartz)} + 2\ Na^+ = 2\ NaAlSi_3O_8 \text{ (albite)} + Ca^{2+}$$

389 The calcium and bicarbonate ions can be often associated with calcite, which is an omnipresent
390 mineral in the hydrothermal reservoirs (Michard, 1985), following the equation:

391 $$Ca^{2+} + HCO_3^- = CaCO_3 \text{ (calcite)} + H^+$$

392 When calcium and pH are controlled by other mineral phases or CO_2 pressure, bicarbonate is
393 then controlled by calcite.

394 In a similar way, increased potassium dissolution with increasing temperature due to K-feldspar
395 dissolution, is also associated with albite precipitation following the chemical reaction:

396 $$KAlSi_3O_8 + Na^+ = NaAlSi_3O_8 + K^+$$

397 This equilibrium reaction explains why the Na-K geothermometer (Fournier, 1979; Giggenbach,
398 1988) gives a relatively good estimate of deep reservoir temperatures for most of the deep Li-
399 rich brines with reservoir temperatures over 120 °C (Fig. 6; Sanjuan *et al.*, 2019). For fully
400 equilibrated geothermal waters in granitic reservoirs, albite controls the Na concentration, while
401 K-feldspar and muscovite fix K and Al contents (Giggenbach, 1997). In addition, the Na-K
402 geothermometers are based on the ion-exchanging equilibrium of Na and K between co-existing
403 alkali feldspars. It is generally recommended to use the Fournier (1979) thermometric
404 relationship for temperature estimations below 200-250 °C, and that of Giggenbach (1988) for
405 higher temperature estimates (Fig. 6).

406 Inversely to the behaviour of aqueous calcium, potassium and silica species, the concentrations
407 of dissolved magnesium and sulphate decrease with increasing temperatures.

Mg concentrations can be controlled by illite (represented by muscovite) and magnesian chlorite precipitation from biotite (represented by phlogopite component) and white micas (represented by Na-mica and pyrophyllite) dissolution, following the chemical reaction:

$$KAlSi_3O_8 \text{ (K-feldspar)} + KAlMg_3Si_3O_{10}(OH)_2 \text{ (phlogopite)} + NaAl_3Si_3O_{10}(OH)_2 \text{ (Na-mica)} + 2\ Al_2Si_4O_{10}(OH)_2 \text{ (pyrophyllite)} + 4\ H_2O + 2\ Mg^{2+} =$$

$$NaAlSi_3O_8 \text{ (albite)} + 2\ KAl_3Si_3O_{10}(OH)_2 \text{ (muscovite)} + Mg_5Al_2Si_3O_{10}(OH)_8 \text{ (chlorite)} + 5\ SiO_2 \text{ (quartz)} + 4\ H^+$$

Secondary anhydrite ($CaSO_4$) precipitation could explain the decrease of sulphate concentrations, as observed at Rittershoffen (Vidal *et al.*, 2018). Secondary barite was noted at Soultz as fracture fillings, mainly in sandstone and some in granite (Genter and Traineau, 1996).

Such chemical reactions (dissolution of plagioclase and K-felspar, albitization of feldspar surfaces, chloritization of biotite, and precipitation of illite, anhydrite) are relatively common in high-temperature geothermal fields, but were especially observed in URG granite alteration processes (Genter, 1989; Ledésert *et al.*, 1996; 1999; Hooijkaas *et al.*, 2006; Vidal *et al.*, 2018). They were also described by Savage *et al.* (1993), Lo Ré *et al.* (2014) and Drüppel *et al.* (2020), from their experimental work on the alteration of granitic rocks by NaCl brines at 200 and 250 °C, and were partly observed in low-temperature tests of water-sandstone interactions carried out by Ludwig *et al.* (2011) and Schmidt *et al.* (2017), at 200 and 260 °C.

For the deep URG Li-rich brines, Sanjuan *et al.* (2010; 2016a) determined that they had a pH of around 5.0 and were close to equilibrium for albite, K-feldspar, quartz, calcite, dolomite, $CaSO_4{:}0.5H_2O$ (β), barite, fluorite, pyrite, Mg-illite, and smectite or montmorillonite at 200-230 °C, with a CO_2 pressure of about 6 bar, based on the brine's chemical composition and on geochemical modelling work.

4. Possible sources and control of lithium in the brines

Although remarkably high fluid-salinity values combined with high temperatures seem to be a proxy for high Li concentrations in geothermal brines, these two parameters alone are not sufficient for explaining the Li enrichment. Several Na-Cl brines in volcanic environments at high-temperatures have low Li concentrations (Sanjuan and Millot, 2009). For example, the geothermal Na-Cl brines (TDS about 120 g/l) in Djibouti, discharged from the Asal basalt reservoir at 260 °C in an arid volcanic area, have rather low Li concentrations (13-14 mg/l; Sanjuan *et al.*, 1990). Similarly, the Na-Cl brine from the Riito well in the Baja California peninsula (Mexico), has a relatively low Li concentration (16 mg/l) in view of its salinity (TDS > 60 g/l) and its temperature at depth (225 °C; Barragan *et al.*, 2001). Other examples, such as geothermal brines in the USA and Iceland, and hydrothermal brines discharged from East Pacific rise, Mid-Atlantic ridge or other ridges at very high-temperatures (Sanjuan and Millot, 2009), can be also mentioned.

4.1 Thermodynamic considerations

In addition to major species such as Na, K, Ca, Mg, SiO_2, HCO_3 and SO_4, for which temperature is the main factor controlling their concentration in solution at medium-to-high temperatures (Reed, 1982; Michard and Roekens, 1983; Reed and Spycher, 1984; Michard, 1985; Spycher *et al.*, 2014), Li concentrations also depend on fluid salinity, the type of reservoir rock, and its mineralogical constituents interacting with the geothermal fluid (Sanjuan *et al.*, 2010; 2014). Consequently, different Na-Li thermometric relationships were determined in the literature following the fluid salinity and type of geological environment (Fouillac and Michard, 1981; Kharaka *et al.*, 1982; Kharaka and Mariner, 1989; Michard, 1990; Sanjuan *et al.*, 2014) and are shown on Figure 7, Na/Li being a molar ratio.

Figure 8, showing Li *versus* Na concentrations and integrating the isotherms calculated with the Na-Li thermometric relationships determined by Fouillac and Michard (1981) for volcanic and

458 crystalline waters with Cl ≥ 0.3 M, by Kharaka *et al.* (1982) for geothermal and hydrocarbon
459 brines in sedimentary basins and Sanjuan *et al.* (2014) for very high-temperature geothermal
460 waters in volcanic environment, indicates that:

461 - the ultra-high temperature (300-380 °C) deep Li-rich brines discharged from
462 metamorphosed Mesozoic volcano-sedimentary rocks in volcanic environments (Cesano
463 and Campi Flegrei in Italy, Salton Sea in USA, etc.) provide relatively good fits to the
464 isotherms determined by the Na-Li thermometric relationship defined by Sanjuan *et al.*
465 (2014);

466 - the low to high temperature (120-235 °C) deep Li-rich brines from tectonic sedimentary
467 basins over crystalline basements (URG in France and Germany, Molasse Basin and
468 Groβ Schönebeck in Germany) follow the isotherms calculated with the Kharaka *et al.*
469 (1982) Na-Li thermometric relationship relatively well;

470 - the very low temperature (close to 52°C) South Crofty mine fluid (UK) does not fit any of
471 the three Na-Li relationships.

472 Figure 8 also shows that the Li concentration of deep brines from the tectonic sedimentary
473 basins over crystalline basements is much higher than that of the brines from volcano-
474 sedimentary environment at equivalent temperature and sodium concentration.

475 For the Na-Li relationship determined by Sanjuan *et al.* (2014) for ultra-high temperature
476 geothermal waters in volcanic environment, and using thermodynamic calculations, these
477 authors suggested that this relationship could be derived from the following chemical reaction
478 (1):

479 $KAlSi_3O_8$ (K-feldspar) + $NaAl_3Si_3O_{10}(OH)_2$ (Na-mica) + $LiAl_3Si_3O_{10}(OH)_2$ (Li-mica) + 2 SiO_2
480 (quartz) + H_2O + Na^+ =

481 2 $NaAlSi_3O_8$ (albite) + $KAl_3Si_3O_{10}(OH)_2$ (muscovite) + $Al_2Si_2O_5(OH)_4$ (kaolinite) + Li^+ (1)

In this study, with similar thermodynamic calculations, we have found that this Na-Li relationship could be also derived from the following chemical reaction (2):

$$KAlSi_3O_8 \text{ (K-feldspar)} + LiAl_3Si_3O_{10}(OH)_2 \text{ (Li-mica)} + Al_2Si_2O_5(OH)_4 \text{ (kaolinite)} + 2\ SiO_2 \text{ (quartz)} + Na^+ =$$

$$NaAlSi_3O_8 \text{ (albite)} + KAl_3Si_3O_{10}(OH)_2 \text{ (muscovite)} + Al_2Si_4O_{10}(OH)_2 \text{ (pyrophyllite)} + H_2O + Li^+ \quad (2)$$

Several same minerals are involved in both reactions, but the one with pyrophyllite as alteration product at high-temperature (metamorphic) conditions seems to be more consistent with the temperature conditions and geological environment. This mineral assemblage seems to be in accordance with the ultra-high temperature reservoirs constituted of metamorphosed Mesozoic sedimentary rocks in volcanic environment as those of the Italian and Salton Sea geothermal areas (Elders and Cohen, 1983).

For the Na-Li relationship determined by Kharaka *et al.* (1982) for geothermal and oilfield brines in sedimentary basins, we carried out the same type of thermodynamic calculations in this study. These calculations leads us to suggest that this relationship could be derived from reaction (3):

$$LiAl_3Si_3O_{10}(OH)_2 \text{ (Li-mica)} + 4\ SiO_2 \text{ (quartz)} + Na^+ = NaAlSi_3O_8 \text{ (albite)} + Al_2Si_2O_{10}(OH)_2 \text{ (pyrophyllite)} + Li^+ \quad (3)$$

In all cases, Li-mica dissolution and albite precipitation are involved, suggesting that the mica mineral phase is the main source of lithium in both environments.

Except for the South Crofty mine fluid that indicates a lower temperature (close to 52 °C) - and probably other (unknown) very low temperature cases -, the Na-K and Na-Li thermometric relationships of Figure 9 show that all Li-rich brines inventoried in this study are in chemical equilibrium with respect to Na- and K-feldspars at relatively high-temperatures and that they come from two only types of geological reservoirs, in which mica dissolution is suspected.

Relative to the geothermal brines discharged from the granite basement in the URG, which have comparable salinity (close to 90 to 100 g/l) and chemical and isotopic characteristics to those of the Buntsandstein brine from the 3400 m-deep Cronenbourg geothermal well in the sedimentary part of the URG (Pauwels *et al.*, 1993; Aquilina *et al.*, 1997), the results shown in Figure 9 are in good agreement with the model of deep fluid circulation proposed by Sanjuan *et al.* (2016a). Taking into account the thermal gradients that can reach 50-60 °C/km in this area (Vernoux and Lambert, 1993; Le Carlier *et al.*, 1994, Aquilina *et al.*, 2000), the deep brines in the granite might have acquired their salinity and much of their chemical and isotopic composition in the Triassic Buntsandstein reservoirs, at high temperatures (225 ± 25 °C) and depths (≥ 4 km) in the centre of the Graben. After that, they would have migrated to the Graben borders *via* the complex network of NW-SE and NE-SW faults (Fig. 3).

At these low temperatures (close to 52 °C), the South Crofty mine fluids are not in full equilibrium with the reservoir rocks. Only the SiO_2 (chalcedony) geothermometer indicates an equilibration temperature close to 54 °C, equivalent to a maximum circulation depth of about 1200 m (Edmunds *et al.*, 1985). Acid hydrolysis of plagioclase and biotite are proposed as the main source of salinity in the Carnmenellis granite groundwaters by these authors. The unusual chemistry combined with the water stable-isotope composition of these fluids riles out seawater and fluid inclusion

4.2 Mineralogical considerations

The thermodynamic considerations that suggest that micas would be the main source of Li for the geothermal brines seem to be in good agreement with the literature mineralogical data analyzed. As mentioned by McDowell and Marshall (1962), Calvet and Prost (1971), Maurel and Volfinger (1977), Chan *et al.* (1992; 2002), Vigier *et al.* (2008), Millot *et al.* (2010), Sanjuan *et al.* (2014), the Li concentrations in deep reservoirs are likely to be dominated by clay minerals, as Li can be incorporated in their octahedral layers.

Octahedral clay minerals, such as montmorillonite, smectite, illite, and chlorite, are some of the essential alteration products of water-rock interactions in geothermal systems (Browne, 1978; Elders and Cohen, 1983; Genter, 1989; Buonasorte *et al.,* 1993; Giggenbach, 1984; Housse, 1984; Fouillac *et al*., 1989; Ledésert *et al*., 1996; 1999; Aquilina *et al*., 1997; Hooijkaas *et al*., 2006; Haffen, 2012; Vidal *et al*., 2018; Duringer *et al*., 2019). Illite or chlorite may also be present in mixed layer clays, and are commonly mentioned as hydrothermal alteration minerals. In parallel, dissolution of white micas, biotite, plagioclase and K-feldspar is frequently observed.

White micas and biotite are among the main carriers of Li in granitic rocks (Li *et al*., 2018b) and in sandstones, especially those resulting from mechanical degradation of the granite basement like in the URG (Duringer *et al*., 2019). After Ogorodova *et al.* (2010), lithium micas are typically related to rare-metal granites and pegmatites, Ta-bearing metasomatic, topaz-lithium granites, and cassiterite-quartz deposits (tin greisens). In different rocks, lithium micas acquire specific composition, structure and properties related to their genetic conditions; they can be considered as mineralogical indicators of the formational affiliation of deposits, and commonly, of definite types of mineralization.

According to Ogorodova *et al.* (2010), lithium micas stand out among layer silicates with interlayer K cations, by the amount and diversity of mineral species. A particular position of lithium micas is related to the presence of lithium cations, which, together with aluminium and ferrous iron, occupy octahedra of 2:1 layers, following a near tri-octahedral law. The lithium micas have a complex variable composition because of common isovalent and heterovalent isomorphic substitutions. In terms of composition, lithium micas were divided by Ogorodova *et al.* (2010) into poor-Fe lithium-aluminium (lepidolite, polylithionite), ferrous lithium (zinnwaldite, protolithionite), and lithium-magnesium (taeniolite, spodiophyllite) groups. There are also very scarce Mn-rich analogues of zinnwaldite, i.e. masutomilite and norrishite.

According to Sturchio and Chan (2003), the mechanism for Li removal is most likely precipitation of minerals (Li incorporation into these alteration minerals), because Li may

557 substitute for Mg in the octahedral sites of phyllosilicates and other alteration minerals (similarity
558 in ionic radii of Li and Mg). Using thermal waters collected from the Biscuit Basin Flow,
559 Yellowstone National Park (USA), Shaw and Sturchio (1992) clearly demonstrated that lithium
560 was preferentially trapped in illitic alteration products with increasing temperature and that,
561 consequently, the retention of this element was favoured by abundant illitic alteration. Similar
562 observations were made by these authors on rhyolites and associated thermal waters collected
563 from the Valles caldera, New Mexico, and from the Inyo Domes chain, in the Long Valley
564 caldera, California (USA).

565 Li can also be scavenged by other clays such as smectites, mixed-layer clays, or chlorite (Chan
566 *et al.*, 1992, 2002; Millot *et al.*, 2010). Numerous authors mentioned by Merceron *et al.* (1987)
567 have described Li-rich chlorite and tosudite (ordered di-octahedral interstratified
568 chlorite/smectite mineral). Li can be adsorbed in the interlayer region of swelling smectite-
569 containing minerals (Zhang *et al.*, 1998), dramatically increasing the Li content of the bulk clay
570 and affecting the overall isotopic composition. In the Cascadia Basin of northwest North
571 America, argillaceous sedimentary units have high Li contents whereas sandy turbidites are low
572 in Li (Chan *et al.*, 2006). Clayey silt there is rich in phyllosilicates (e.g., smectite, chlorite, illite,
573 muscovite), whereas sand and silt are rich in feldspars. However, in the hydrothermally altered
574 sedimentary units in the Middle Valley of the Juan de Fuca Ridge, studied by Decitre *et al.*
575 (2004), where alteration clays such as illite, smectite, corrensite, swelling chlorite, talc and
576 micas were investigated at different depths, Li is more abundant (50-76 ppm) when illite and
577 chlorite are present. When only abundant smectite was detected, Li concentrations were lower
578 (13 ppm).

579 In core samples from the URG granite, petrographic study shows that organic matter is
580 exclusively associated with tosudite, which is mainly observed in relics of plagioclase grains,
581 progressively altered through interaction with Li-bearing hydrothermal fluids percolating in the
582 granite fractures (Ledésert *et al.*, 1996, 1999; Bartier *et al.*, 2008). Biotite is then locally

583 replaced by chlorite, carbonates and illite. Ledesert *et al.* (1996) clearly show the occurrence of
584 specific secondary clay minerals bearing lithium in the damaged zone of a permeable fault in
585 the Soultz granite. This clay bearing lithium was spatially associated to the occurrence of
586 organic matter in the faulted and altered basement.

587 To conclude, the above observations are in good agreement with a process of dissolution of
588 white mica and biotite as main source of Li for geothermal brines. However, they also suggest
589 that a part of Li could be also preferentially incorporated into illite, chlorite or tosudite structures
590 related to alteration products. Considering these mineralogical points, the analysis of δ^7Li values
591 for aqueous Li (see 4.3, hereafter) can be a very useful tool for identifying which reservoir
592 minerals interact with the geothermal fluids.

593 **4.3 Li-isotope considerations**

594 Due to the absence of Li-isotope data for most of the deep Li-rich brines of the BRGM-EIFER
595 database, only the Li-rich brines from the Upper Rhine Graben (URG) could be studied and
596 discussed. The δ^7Li values in these brines display a narrow range from +1.0‰ to +1.7‰
597 (Sanjuan *et al.*, 2016a). Similar δ^7Li values (-0.4‰, -0.1‰ and +0.6‰) were reported for the
598 Soultz-sous-Forêts geothermal brines by Sanjuan *et al.* (2010). These lithium-isotopic
599 signatures agree with the Upper Continental Crust signature as reported by Teng *et al.* (2004),
600 with δ^7Li = 0‰ ± 2. Sanjuan *et al.* (2016a) observed that these Li-isotopic signatures are very
601 different from the equivalent marine signatures of +31 ± 0.5‰ (Millot *et al.*, 2010).

602 The latter, in their study dealing with water-rock interactions at temperatures ranging from 25 to
603 250 °C, experimentally determined a relationship of Li isotope fractionation between solution
604 and solid to be a function of temperature ($\Delta_{\text{solution - solid}} = 7847 / T(K) - 8.093$). This gave a Li-
605 isotope fractionation between brine and rock ($\Delta_{\text{solution - solid}}$) value close to +7.7‰ at 225 °C.

606 Isotopic fractionation factors inferred from studies of altered basalt and hydrothermal solutions
607 indicate similar (slightly lower) values for $\Delta_{\text{solution - solid}}$ (Chan and Edmond, 1988; Chan *et al.*,

608 1992, 1993, 1994; James et al., 1999), with Li-isotope fractionation ($\Delta_{solution - solid}$) values close to
609 +6.9‰ at 225 °C.

610 Consequently, considering the recorded δ^7Li values of the Li-rich URG brines (-0.4‰ to +1.7‰)
611 and assuming similar isotope fractionation, it can be estimated that the δ^7Li values of the rock in
612 equilibrium with these brines vary from -8.1‰ to -5.2‰. Such values are not characteristic of
613 granite (δ^7Li from -2‰ to +2‰), but rather correspond to sedimentary rock (Coplen *et al.*, 2002).
614 A similar conclusion had already been drawn by Sanjuan *et al.* (2010) for the Soultz-sous-Forêts
615 geothermal fluids. Sanjuan *et al.* (2016a) suggested that a major part of the high Li
616 concentrations of Li-rich URG brines could well be due to the dissolution of micas. The
617 laboratory work by Martin *et al.* (2015) about *in situ* lithium and boron isotope determinations by
618 LA-MC-ICP-MS, showed that the δ^7Li values in mica from a mica-albite rock (from -6.0‰ to 5‰)
619 are compatible with those previously estimated (-8.1‰ to -5.2‰) from the URG Li-rich brines
620 using the relationship of Li-isotope fractionation between brine and rock. These micas could
621 derive from Triassic Buntsandstein micaceous sandstone, which partly results from the
622 mechanical degradation of the granite basement (Duringer *et al.*, 2019) and Hercynian massifs.
623 Augustsson *et al.* (2018) have shown that particularly rocks from the Variscan Orogen of the
624 Massif Central and Bohemian Massif also contributed to the Lower and Middle Buntsandstein
625 subgroups in the German Basin.

626 According to Duringer et al. (2019), the Buntsandstein consists mainly of a 450 m thick
627 continental red sandstone that is fine to coarse-grained with some conglomeratic beds. The
628 Buntsandstein is subdivided into eight formations with thicknesses varying from 10 to 100 m.
629 Several sandstones (Grès d'Annweiler in the Lower Buntsandstein, Couches Intermédiaires and
630 Grès à Voltzia in the Upper Buntsandstein) are constituted of micaceous and clayey fine-to
631 medium-grains. The top of many Grès à Voltzia is particularly rich in micas (Duringer *et al.*,
632 2019; Aichholzer *et al.*, 2019). According to Mosser *et al.* (1971), the Grès à Voltzia, collected
633 from the northern part of the Vosges, are made up of 45-60% quartz, 20-30% microcline, 1-3%

muscovite, about 1% biotite, 3-5% pelitic cement, and 10-15% micro-stones of quartzites, phyllitic piles and different accessory minerals. The fine fraction of these detrital sedimentary units is very often constituted of nearly pure illite. In biotite and muscovite, the Li concentrations range from 200 to 450 ppm whereas in illite, these concentrations are lower than 150 ppm (Mosser *et al.*, 1971).

The Cronenbourg geothermal well (about 3400 m deep), drilled in 1980, has intersected an apparent thickness of 465 m of Buntsandstein sandstone and 54 m of Permian sandstone (Housse, 1984; Haffen, 2012).

The Buntsandstein formations consist of:

- fine grained red micaceous and clayey sandstones, with interbeds of silt, kaolinite and micaceous reddish clays, between depths of 2701 and 2751 m;
- fine to coarse-grained red micaceous and clayey sandstones with some conglomeratic beds and intercalations of silt, kaolinite and micaceous reddish clays, between depths of 2751 and 2937 m;
- medium reddish and little consolidated between depths of 2937 and 3027 m;
- medium red sandstones with thin intercalations of medium grey, siliceous to quartz sandstones and thin layers of brown-red coloured micaceous clays between depths of 3027 and 3166 m.

Between depths of 3166 and 3220 m, the Permian formations are made up of medium to conglomerate red sandstones, with thin intercalations of medium grey, siliceous to quartz sandstones and thin layers of brown-red coloured micaceous clays.

On the other hand, the work by Clauer *et al.* (2018) on illitization decrypted by B and Li isotope geochemistry of nanometer-size illite crystals from bentonite beds in the East Slovak Basin, indicated that the younger illite crystals contain increasing Li contents (up to 140 µg/g), with decreasing δ^7Li values (from -7 to -22 ‰). The highest values are close to those estimated from

659 the Li-rich URG brines and are compatible with the fact that illite precipitation can partially
660 remove Li from these brines at about 225 °C.

661 Finally, the Li isotopic signatures of Li-rich URG brines thus seem to agree with a fluid signature
662 mainly derived from high-temperature (225 ± 25 °C) water-rock interactions, mica dissolution
663 and albite and illite precipitation, mainly in the up to 450-m-thick Buntsandstein micaceous
664 continental sandstone and less in the granite basement, with a fluid whose origin is a seawater-
665 derived brine end-member diluted by meteoric water.

666 The lower Li concentrations analysed in experimental NaCl solutions in contact with granite and
667 monzonite at 200 °C (Savage *et al.,* 1993; Drüppel *et al.,* 2020), when compared to geothermal
668 URG brines, suggest that the source of Li from the granite basement is not sufficient to explain
669 the Li concentrations observed in these geothermal brines. In contrast, the high Li concentration
670 determined in the Cronenbourg fluid (210 mg/l), which is only in contact with the Buntsandstein
671 sandstone and has a similar geochemical composition than that of the geothermal brines from
672 the granite basement, seems to agree with the fact that most of the Li comes from the
673 Buntsandstein sandstone alteration, even if alteration of the granite basement can represent
674 another potential source of lithium. Laboratory experiments on sandstone alteration with NaCl
675 brines at 200 °C, similar to those carried out by Schmidt *et al.* (2017), but integrating Li chemical
676 and isotope analyses, might confirm the Buntsandstein as the main lithium source.

677 **4.4 Future direction: Li resource assessment**

678 As mentioned above, the Upper Rhine Graben (URG) area along the French/German border
679 hosts several geothermal projects, in operation or under development, and may be the most
680 promising zone for geothermal Li mining in Europe. Though the Li concentrations in brines of
681 the URG sites are relatively well known, production-fluid flow-rates and injectivity indices, the
682 circulation of deep fluids in the complex fault networks, and their volume and recharge areas,
683 remain poorly defined, but essential parameters in this fractured environment.

Based on current technical and scientific knowledge, it is difficult to assess the Li resource in the geothermal reservoirs of the URG area, such evaluation being the key parameter for deciding upon Li exploitation here. Considering: 1) a mean concentration of aqueous Li of 155 mg/l; 2) pessimistic and optimistic assumptions about the "useful reservoir volume"; 3) the porosity of the Buntsandstein and Muschelkalk geothermal aquifers in a 30 x 30 km area, Pauwels *et al.* (1991) estimated the Li resource at 300,000 to 2,200,000 tons of lithium metal. The volume of fluid circulating in the granite basement was not integrated in these calculations.

These values, based on the existence of a porous medium, can be considered as encouraging first-order evaluations of the potential Li resource in the Upper Rhine Graben area, given that:

- the potential of dissolved Li in brines circulating in the granite was not recognized;
- the prospective Li volume that may be dissolved from rock during reinjection of the Li-depleted brines into the geothermal reservoir, was not considered.

Nevertheless, these evaluations, based on information of thirty years ago, now known to be highly incomplete and inadequate, are not representative of the dissolved lithium that may be really extracted from the geothermal brines circulating in a fractured medium such as that of the Upper Rhine Graben. To obtain a more accurate estimate of the amount of available Li, and of the sustainable use and long-term capacity of the reservoir, it is necessary to work at the scale of a site rather than at a regional scale. It is thus important to know the location, size and geometry of the main faults, fractures, geological discontinuities, etc., in which the deep geothermal brines can circulate. To this end, 3D-geological models of the URG Triassic geothermal reservoirs are in construction with the Geomodeller code (Dezayes, 2007; Dezayes *et al.*, 2011), which must be refined through integration of all recent data, such as those compiled by Haffen (2012).

In this type of model, two key parameters are:

- the estimated fracture density in the studied area;

- the percentage of tectonic structures and geological discontinuities through which the deep brines really circulate.

In order to minimize the uncertainty concerning extractable Li volumes and to obtain the most realistic values, we now recommend to work at the scale of individual geothermal sites (Soultz-sous-Forêts, Rittershoffen, etc.). Here, hydrodynamic parameters and fluid-circulation patterns are better constrained than at a regional scale, thanks to the data obtained during drilling of the deep heat-exchanger wells, the fluid-production and inter-well fluid-circulation tests, and the associated tracer tests (Sanjuan *et al.*, 2006, 2015, 2016b; Dezayes *et al.*, 2010; Gentier *et al.*, 2011; Radilla *et al.*, 2012; Baujard *et al.*, 2017; Vidal *et al.*, 2018). Even if the site of Soultz-sous-Forêts is probably the best-documented geothermal area in the Upper Rhine Graben (Sanjuan *et al.*, 2019), more knowledge and numerical modelling is still needed to better understand the circulation of deep fluids and estimate the volume that they represent.

Subsequently, the integration of hydrothermal and geochemical numerical models into geological models (especially of fault networks), should provide additional hydraulic and geochemical constraints for obtaining more realistic evaluations of the dissolved Li resources extractable from the geothermal brines. It is clear that such Li resources will depend on the different characteristics of each geothermal site (flow-rates of discharged and injected fluids, porosity and permeability, reservoir volume, inter-well connections, fluid-circulation paths, concentrations of aqueous Li, sources of Li supply, possible Li recharge, etc.), and may be relatively variable between sites.

Assuming that the current and short-term planned geothermal projects of the URG area will produce brines for a long time with the presently known Li concentrations and production flow-rates, it was estimated that these projects could generate a potential lithium production of 4,000 to 6,000 tons per year from geothermal brines (Sanjuan *et al.*, 2020). This corresponds to an annual turnover of 21,300 to 32,000 t/year of lithium carbonate equivalent (LCE). However, for sustainable Li exploitation, it is essential to estimate the long-term behaviour of capacity, and

735 the economic and technical conditions of exploitation for each geothermal site in terms of Li
736 production, to render these estimations feasible.

737

738 ## 5. Conclusions

739 Among all known European geothermal and hydrocarbon fields reviewed in the literature so far,
740 six main geothermal areas were detected whose deep fluids contain high Li concentrations,
741 ranging from 125 to 480 mg/l, in Italy, Germany, France and the United-Kingdom.

742 This study shows that the URG area straddling the French/German border, which currently
743 hosts several geothermal projects in operation or under development, is probably one of the
744 most promising European zones for geothermal lithium extraction from brines in terms of Li
745 resources. If geothermal brines can provide much needed local Li resources for Europe with a
746 zero-carbon process, lithium production could also improve the business models of geothermal-
747 energy projects, which today are mainly based on heat and/or electricity sales. After
748 presentation and discussion about the main geochemical characteristics of the European Li-rich
749 geothermal brines, this study has also contributed to identify their main source of Li, which was
750 poorly known, and to understand natural processes of lithium enrichment, as the influence of
751 temperature, fluid salinity and nature of the reservoir rocks.

752 Water-rock interaction processes at relatively high temperatures (≥ 120 °C) are the dominant
753 source and control of these high Li contents in the deep fluids, but other important features
754 govern these contents as well. They include the type of reservoir rock and all the processes that
755 can influence the salinity of such fluids, especially their Na and Cl concentrations, like seawater
756 or freshwater evaporation during arid-climate periods, halite dissolution by dilute waters, mixing
757 of saline and dilute waters, low-temperature weathering, formation of transition zone brines, in
758 sedimentary basins, or contributions of primary neutralization brines - or parent geothermal
759 fluids - in active volcanic environments.

760 The two Na-Li thermometric relationships used in this study, defined for two different geological
761 environments in the literature (sedimentary basins and volcanic environment), indicate that high
762 initial Na concentrations and temperatures are required for obtaining high Li concentrations.
763 However, for a same Na concentration, temperature must be higher in the volcanic environment
764 than in sedimentary basins to have an equivalent Li concentration. All the deep brines are in
765 chemical equilibrium with respect to albite and K-feldspar at their reservoir temperature,
766 controlling the Na and K concentrations in solution.

767 In this study, the South Crofty mine fluid in the UK, was the only known example of Li-rich water
768 (about 125 mg/l) to have a relatively low salinity (TDS ≈ 19 g/l), indicating a low reservoir
769 temperature, close to 52 °C. This fluid is not fully in chemical equilibrium with the host granite
770 and only its SiO_2 concentration corresponds to an equilibrium with respect to chalcedony at this
771 temperature.

772 The Li concentrations in geothermal brines at temperatures over 120 °C seem to be mainly
773 controlled by the presence of clay minerals, as lithium is easily incorporated in their octahedral
774 layers. Thermodynamic considerations derived from Na-Li thermometric relationships and Li-
775 isotope fractionation data suggest that the main source of Li would be white mica and biotite
776 dissolution. Part of this lithium could also be fixed by hydrothermal alteration clays like illite,
777 chlorite, tosudite, etc., depending on the characteristics of the geothermal reservoirs such as
778 their temperature, fluid salinity, and mineralogical composition.

779 For the URG brines, the major source and control of lithium probably is the fractured and
780 permeable Triassic Buntsandstein micaceous continental sandstone, with a thickness of up to
781 450 m, boosting the economic interest and sustainability of Li exploitation from these fluids. A
782 major part of Li would come from mica dissolution and could be further controlled by illite,
783 chlorite or tosudite precipitation at about 225 °C. Alteration of the fractured granite basement,
784 which contains similar minerals interacting with brines, could be another - though smaller -

source of lithium, as suggested by recent experimental studies of granite-brine interaction at temperatures of up to 200 °C.

Under this scenario, the Li reserves and their lifetime appear to be much higher than was initially assumed. It is also probable that reinjection of the Li-depleted brine into the underground, after Li extraction, will have a reduced medium- to long-term effect on the Li concentration of the remaining geothermal reservoir brine - in chemical and isotope equilibrium with mica and illite at 225 °C - through new Li input from mica into the reservoir brine. To confirm the rare data on this aspect and to make better estimates of the Li reserves, it will be necessary to carry out further mineralogical, chemical and isotope analyses on the Buntsandstein sandstones as well as on unaltered and altered granite samples.

The Li-concentration values of these brines (≥ 150 mg/l) do not seem to be the limiting factor for geothermal Li exploitation. To arrive at an optimal estimation of the Li resource of these brines, we must, however, evaluate the reservoir volume of these geothermal brines, and obtain a better understanding of their origin, recharge and deep circulation in fractured rocks. The sources of the lithium supply (which may be site specific for each geothermal site), the optimization of the lithium extraction process, and a thorough evaluation examination of the economic conditions of its exploitation are further key parameters that will require much more work for the development of this type of Li exploitation.

Acknowledgments

This work, performed within the framework of the EuGeLi project (European Geothermal Lithium brines), coordinated by ERAMET IDEAS, was co-funded by the European Union, under the European Institute of Technology (EIT) Raw Materials Program, by BRGM, the French Geological Survey, and by EDF (Électricité de France S.A.). We thank Clio Bosia and Albert Genter (ES-Géothermie) for their fruitful discussions and relevant comments during the EuGeLi project. We would also like to acknowledge Romina López Steinmetz and Oleg Pokrovsky for

their remarks and comments in a previous version of this manuscript, and two anonymous reviewers for the present version of this manuscript. H.M. Kluijver revised the English of this manuscript.

References

Aichholzer C., Duringer Ph., Genter A. (2019) - Detailed descriptions of the Lower-Middle Triassic and Permian formations using cores and gamma-rays from the EPS-1 exloration geothermal borehole (Soultz-sous-Forêts, Upper Rgine Graben, France). *Geothermal Energy*, 7:34, 28 p. https://doi.org/10.1186/s40517-019-0148-1.

Alekseeva L.P., Alekseev S.V. (2018) - Industrial groundwater of the Olenek Artesian Basin: Geochemistry and development prospects. *Water Resources,* 45, n° 1, 79-88. *Original Russian text published in Vodnye Resursy, 2018, vol. 45, n°1*, 42-51.

Aquilina L., Pauwels H., Genter A., Fouillac C. (1997) - Water-rock interaction processes in the Triassic sandstone and the granitic basement of the Rhine Graben: Geochemical investigation of a geothermal reservoir. *Geochim. Cosmochim. Acta*, 61, n° 20, 4281-4295.

Aquilina L., Genter A., Elsass Ph., Pribnow D. (2000) - Evolution of fluid circulation in the Rhine Graben: constraints from the chemistry of the present fluids. *In: I. Stober & K. Bucher (eds.), Hydrogeology of Crystalline Rocks, Chapter 4. Kluwer Academic Publishers, Dordrecht,* 177-203.

Augustsson C., Voigt Th., Kristin B., Kreißler M., Gaupp R., Gärtner A., Hofmann M., Linnemann U. (2018) - Zircon size-age sorting and source-area effect: The German Triassic Buntsandstein Group. *Sedimentary Geology*, 375, 218-231.

833 Barberi F., Buonasorte G., Cioni R., Fiordalisi A., Foresi L., Iaccarino S., Laurenzi M.A., Sbrana
834 A., Vernia L., Villa I.M. (1994) - Plio-Pleistocene geological evolution of the geothermal area
835 of Tuscany and Latium. *Mem. Descr. Carta Geol. d'Italia*, 49, 77-134.

836 Barragan R.M., Birkle P., Portugal E., Arellano V.M., Alvarez J. (2001) - Geochemical survey of
837 medium temperature geothermal resources from the Baja California Peninsula and Sonora,
838 México. *J. Volcanol. Geotherm. Res.*, 110, 101-119.

839 Barrett W.T., O'Neill B.J.Jr. (1970) - Recovery of lithium from saline brines using solar
840 evaporation. *In Rau J.L., Dellwig L.E. Eds., Third Symposium on Salt: Northern Ohio*
841 *Geological Society, v. 2*, 47-50.

842 Bartier D., Ledésert B., Clauer N., Meunier A., Liewig N., Morvan G., Addad A. (2008) -
843 Hydrothermal alteration of the Soultz-sous-Forêts granite (Hot Fractured Rock geothermal
844 exchanger) into a tosudite and illite assemblage. *Eur. J. Mineral.*, 20, 131-142.

845 Baujard C., Genter A., Dalmais E., Maurer V., Hehn R., Rosillette R., Vidal J., Schmittbuhl J.
846 (2017) - Hydrothermal characterization of wells GRT-1 and GRT-2 in Rittershoffen, France:
847 implications on the understanding of natural flow systems in the Rhine Graben. *Geothermics*,
848 65, 255-268.

849 Bertleff B., Joachim H., Koziorowski G., Leiber J., Ohmert W., Prestel R., Stober I., Strayle G.,
850 Villinger E., Werner J. (1988) - Ergebnisse der Hydrogeothermiebohrungen in Baden-
851 Württemberg. *Jh Geol. Landesamt Baden-Württemb*, 30, 27-116.

852 Birkle P., Portugal Marin E., Barragán Reyes R.M. (2010) - Chemical-isotopic evidence for the
853 origin of geothermal fluids at the Las Tres Vírgenes Geothermal field, BC, NW-México. *Proc.*
854 *World Geothermal Congress 2010, Bali, Indonesia, 25-29 April 2010*, 10 p.

855 Blake R.L. (1974) - Extracting minerals from geothermal brines: A literature Study. *U.S.*
856 *Department of the Interior, Bureau of Mines, Information Circular 8638,* 25 p.

857 Bosia C., Mouchot J., Ravier G., Seibt A., Jänichen S., Degering D., Scheiber J., Dalmais E.,
858 Baujard C., Genter A. (2021) - Evolution of brine geochemical composition during operation
859 of EGS geothermal plants (Alsace, France). *Proc. 46th Workshop on Geothermal Reservoir*
860 *Engineering, Stanford University, California, February 15-167, 2021,* 21 p.

861 Bradley D., Munk L. A., Jochens H., Hynek S., Keith L. (2013) - A preliminary deposit model for
862 lithium brines. *U.S. Geological Survey Open-File Report 2013-1006*, 6 p.

863 Browne P.R.L. (1978) - Hydrothermal alteration in active geothermal fields. *Annual Review of*
864 *Earth and Planetary Sciences*, 6 (1), 229-248.

865 Buonasorte G., Cameli G.M., Fiordelisi A., Parotto M., Perticone I. (1993) - Results of
866 geothermal exploration in Central Italy (Latium-Campania). *Proc. World Geothermal*
867 *Congress, Florence, Italy, 28-31 May 1995*, 1293-1298.

868 Calamai A., Cataldi R., Dall'Aglio M., Ferrara G.C. (1976) - Preliminary report on the Cesano hot
869 brine deposit (Northern Latium, Italy). *Proc. 2nd U.N. Symposium on the Development and*
870 *Use of Geothermal Energy, S. Francisco, USA*, 305-313.

871 Calvet R., Prost R. (1971) - Cation migration into empty octahedral sites and surface properties
872 of Clays. *Clays and Clay Min.*, 19, 175-186.

873 Carella R., Guglielminetti M. (1983) - Multiple reservoirs in the Mofete field, Naples, Italy. *Proc.*
874 *9th Workshop on Geothermal Reservoir Engineering, Stanford University, California, 13-15*
875 *December 1993*.

876 Chan L.H., Edmond J.M. (1988) - Variation of lithium isotope composition in the marine
877 environment: a preliminary report. *Geochim. Cosmochim. Acta*, 52, 1711-1717.

878 Chan L.H., Edmond J.M., Thompson G., Gillis K. (1992) - Lithium isotopic composition of
879 submarine basalts: implications for the lithium cycle in the oceans. *Earth Plan. Sci. Lett.*, 108,
880 151-160.

881 Chan L.H., Edmond J.M., Thompson G. (1993) - A lithium isotope study of hot springs and
882 metabasalts from mid-ocean ridge hydrothermal systems. *J. Geophys. Res.*, 98, 9653-9659.

883 Chan L.H., Gieskes J.M., You C.F., Edmond J.M. (1994) - Lithium isotope geochemistry of
884 sediments and hydrothermal fluids of the Guaymas Basin, Gulf of California. *Geochim.*
885 *Cosmochim. Acta*, 58, 4443-4454.

886 Chan L.H., Alt J.C., Teagle A.H. (2002) - Lithium and lithium isotope profiles through the upper
887 oceanic crust: a study of seawater-basalt exchange at ODP Sites 504B and 896A. *Earth*
888 *Plan. Sci. Lett.*, 201, 187-201.

889 Chan L.H., Leeman W.P., Plank T. (2006) - Lithium isotopic composition of marine sediments.
890 *Geochemistry, Geophysics, Geosystems (G3, electronic journal of Earth Sciences)*, 7, n°6,
891 25 p.

892 Cinti D., Procesi M., Tassi F., Montegrossi G., Sciarra A., Vaselli O., Quattrocchi F. (2011) -
893 Fluid geochemistry and geothermometry in the western sector of the Sabatini Volcanic
894 District (SVD) and the Tolfa Mountains (Central Italy). *Chem. Geol.*, 284, 160-181.

895 Cinti D., Tassi F., Procesi M., Brusca L., Cabassi J., Capecchiacci F., Delgado Huertas A., Galli
896 G., Grassa F. , Vaselli O., Voltattorni N. (2017) - Geochemistry of hydrothermal fluids from
897 the eastern sector of the Sabatini Volcanic District (central Italy). *Applied Geochemistry*, 187-
898 201.

899 Clauer N., Williams L.B., Lemarchand D., Floriand P., Hontye M. (2018) - Illitization decrypted
900 by B and Li isotope geochemistry of nanometer-sized illite crystals from bentonite beds, East
901 Slovak Basin. *Chem. Geol.*, 477, 177-194.

902 Cocherie A., Guerrot C., Fanning C.M., Genter A. (2004) - Datation U-Pb des deux faciès du
903 granite de Soultz (Fossé rhénan, France). *C.R. Géoscience*, 336, 775-787.

904 Collins A.G. (1975) - Geochemistry of oil field waters. *Elsevier.*

905 Connolly C.A., Walter I.M., Baadsgaard, Longstaffe F.J. (1990) - Origin and evolution of
906 formation waters, Alberta Basin, Western Canada Sedimentary Basin. I. Chemistry. *Appl.*
907 *Geochem.*, 5, 375-395.

908 Coplen T.B., Hopple J.A., Böhlke J.K., Peiser H.S., Rieder S.E., Krouse H.R., Rosman K.J.R.,
909 Ding T., Vocke R.D.Jr., Révész K.M., Lamberty A., Taylor P., De Bièvre P. (2002) -
910 Compilation of minimum and maximum isotope ratios of selected elements in naturally
911 occurring terrestrial materials and reagents. *U.S.G.S. Water-Resources Investigations*
912 *Report 01-4222*.

913 Davis J.R., Friedman I., Gleason J.D. (1986) - Origin of the lithium-rich brine, Clayton Valley,
914 Nevada. *U.S.G.S. Bulletin 1622, Shorter Contributions to Isotope Research*, *Chap. L*, 131-
915 138.

916 Decitre S., Buatier M., James R. (2004) - Li and Li isotopic composition of hydrothermally
917 altered sediments at Middle Valley, Juan De Fuca. *Chem. Geol.*, 211, 363-373.

918 Dezayes C., Genter A., Hooijkaas G.R. (2005) - Deep-seated geology and fracture system of
919 the EGS Soultz reservoir (France) based on recent 5 km depth boreholes. *Proc. World*
920 *Geothermal Congress*, Turkey, 2005.

921 Dezayes Ch., Thinon I., Courrioux G., Tourlière B., Genter A. (2007) - Estimation du potentiel
922 géothermique des réservoirs clastiques du Trias dans le Fossé rhénan. *Final report*
923 *BRGM/RP-55729-FR*, 72 p.

924 Dezayes Ch., Genter A., Valley B. (2010) - Overview of the fracture network at different scales
925 within the granite reservoir of the EGS Soultz site (Alsace, France). *In Proc. World*
926 *Geothermal Congress 2010, Bali, Indonesia, 25-29 April 2010*, 12 p.

927 Dezayes Ch, Beccaletto L., Oliviero G., Baillieux P., Capar L., Schill E. (2011) - 3-D visualisation
928 of a fractured geothermal field: The example of the EGS Soultz site (Northern Upper Rhine

Graben, France). *Proc., 36th Workshop on Geothermal Reservoir Engineering, Stanford University, Stanford, California, January 31 - February 2, 2011, SGP-TR-191*, 6 p.

Drüppel K., Stober I., Grimmer J.C., Mertz-Kraus R. (2020) - Experimental alteration of granitic rocks: implications for the evolution of geothermal brines in the Upper Rhine Graben, Germany. *Geothermics*, 88, 101903, 28 p.

Duringer Ph., Aichholzer C., Orciani S., Genter A. (2019) - The complete lithostratigraphic section of the geothermal wells in Rittershoffen (Upper Rhine Graben, eastern France): a key for future geothermal wells. *BSGF - Earth Sciences Bulletin 2019, Soc. Géol. France, 190, 23 p., Published by EDP Sciences 2019 https://doi.org/10.1051/bsgf/2019012.*

Edmunds W.M., Kay R.L.F., McCartney R.A. (1985) - Origin of saline groundwaters in the Canmenellis granite (Cornwall, England): natural processes and reaction during hot dry rock reservoir circulation. *Chem. Geol.*, 49, 287-301.

Elders W.A., Cohen L.H. (1983) - The Salton Sea geothermal field, California, as a near-field natural analog of a radioactive waste repository in salt. *Technical report BMI/ONWI-513, DE84 003851*, 146 p.

Elert K.H., Henning I., Knabe H.J. (1988) - Untertägige Erdöl-Vorkommen und ihre bergbausicherheitliche Beurteilung. *Z. Angew. Geol.*, 34, 139-144.

Ericksen G.E., Salas R. (1987) - Geology and resources of salars in the central Andes. *U.S.G.S. Open File Rep. 88-210*, 51 p.

Fontes J.-Ch, Matray J.-M. (1993) - Geochemistry and origin of formation brines from the Paris Basin, France. 2. Saline solutions associated with oil fields. *Chem. Geol.*, 109, 177-200.

Fouillac Ch., Michard G. (1981) - Sodium/lithium ratio in water applied to geothermometry of geothermal reservoirs. *Geothermics*, 10, 55-70.

952 Fouillac A.-M., Fouillac Ch., Cesbron F., Pillard F., Legendre O. (1989) - Water-rock interaction
953 between basalt and high-salinity fluids in the Asal Rift, Republic of Djibouti. *Chem. Geol.*, 76,
954 271-289.

955 Fournier R.O. (1979) - A revised equation for the Na/K geothermometer. *Geotherm. Res.*
956 *Counc. Trans.*, 3, 221-224.

957 Fulignati P. (2020). Clay Minerals in Hydrothermal Systems. *Minerals*. 10. 919. 10.3390/
958 min10100919.

959 Garcia M.G., Borda L.G., Godfrey L.V., Lopez Stenmeitz R.L., Losada-Calderon A. (2021) -
960 Characterization of lithium cycling in the Salar De Olaroz, Central Andes, using a
961 geochemical and isotopic approach. *Chem. Geol., 531, 119340.*

962 Garrett D.E. (2004) - Handbook of Lithium and Natural Calcium Chloride. *Elsevier*, 488 p.

963 Genter A. (1989) - Géothermie roches chaudes sèches : le granite de Soultz-sous-Forêts (Bas-
964 Rhin, France), fracturation naturelle, altérations hydrothermales et interaction eau-roche.
965 *Ph.D. thesis, University of Orléans, France*, 191 p.

966 Gentier S., Rachez X., Peter M., Blaisonneau A., Sanjuan B. (2011) - Transport and flow
967 modelling of the deep geothermal exchanger between wells at Soultz-sous-Forêts (France).
968 *Proc. Geothermal Research Council (GRC) Ann. Mtg., San Diego, USA, October 2011*, 12 p.

969 Giggenbach W.F. (1984) - Mass transfer in hydrothermal alteration systems-A conceptual
970 approach. *Geochim. Cosmochim. Acta*, 48 (12), 2693-2711.

971 Giggenbach W.F. (1988) - Geothermal solute equilibria. Derivation of Na-K-Mg-Ca
972 geoindicators. *Geochim. Cosmochim. Acta*, 52, 2749-2765.

973 Giggenbach W.F. (1992) - Magma degassing and mineral deposition in hydrothermal systems
974 along convergent plate boundaries. *Econ. Geol.*, 87, 1927-1944.

975 Giggenbach W.F. (1997) - The origin and evolution of fluids in magmatic-hydrothermal systems.
976 *Geochemistry of Hydrothermal Ore Deposits*, 737-796.

977 Godfrey L.V., Chan L.H., Alonso R.N., Lowenstein T.K., McDonough W.F., Houston J., Li J.,
978 Bobst A., Jordan T.E. (2013) - The role of climate in the accumulation of lithium-rich brine in
979 the Central Andes. *Appl. Geochem.*, 38, 92-102.

980 Gourcerol B., Gloaguen E., Melleton J., Tuduri J., Galiegue X. (2019) - Re-assessing the
981 European lithium resource potential. A review of hard-rock resources and metallogeny. *Ore*
982 *Geol. Rev.*, 109, 494-519, https://doi.org/10.1016/j.oregeorev.2019.04.015.

983 Gourcerol B., Millot R., Gloaguen E., Sanjuan B., Lefebvre G., Bertrand G., Melleton J. (2021) -
984 Overview and re-assessment of the lithium resources in Europe, BRGM expertise on hard
985 rock and geothermal Li. *Critical Minerals Forum - Europe and Africa session, 19th February*
986 *2021*, presentation online.

987 Grimmer J. C., Ritter J. R. R., Eisbacher G. H., Fielitz W. (2017) - The Late Variscan control on
988 the location and asymmetry of the Upper Rhine Graben. *Internat. J. of Earth Sci.*, 106(3),
989 827-853.

990 Haffen S. (2012) - Caractéristiques géothermiques du reservoir gréseux du Buntsandstein
991 d'Alsace. *Ph.D. thesis, Earth Sciences, University of Strasbourg*, 387 p. NNT:
992 2012STRAH004, tel-0078094.

993 Hedenquist J.W (1995) - The ascent of magmatic fluid: Discharge versus mineralization.
994 *Chapter 13, Magmas, fluids, and ore deposits. Editor F.F.H. Thompson, Mineralogical*
995 *association of Canada, Short course series, Victoria, British Columbia, vol. 23*, 263-289.

996 Helvaci C., Mordogan H., Colak M., Gündoga I. (2003) - Presence and distribution of lithium in
997 borate deposits and some recent lake waters of West-Central Turkey. *Int. Geol. Rev.*, 45,
998 14 p.

999 Herrmann A.G. (1961) - Über das Vorkommen einiger Spurenelemente in Salzlösungen aus
1000 dem deutschen Zechstein. *Kali Steinsalz*, 3, 209-220.

1001 Hooijkaas G.R., Genter A., Dezayes Ch. (2006) - Deep-seated geology of the granite intrusions
1002 at the Soultz EGS site based on data from 5 km-deep boreholes. *Geothermics*, 35, 484-506.
1003 https://doi.org/10.1016/ j.geothermics.2006.03.003.

1004 Housse B.A. (1984) - Reconnaissance du potentiel géothermique du Buntsandstein à
1005 Strasbourg-Cronenbourg. *Geothermie Actualités*, 1, 36-42.

1006 Hurtig E., Cermak V., Haenel R., Zui V. (1992) - Geothermal Atlas in Europe. *Hermann Haak*
1007 *Eds, Germany*.

1008 Jagoutz E., Palme H., Baddenhausen H., Blum K., Cendales M., Dreibus G., Spettel B., Lorenz
1009 V., Wänke H. (1979) - The abundances of major, minor and trace elements in the earth's
1010 mantle as derived from primitive ultramafic nodules. *In: Lunar and Planetary Science*
1011 *Conference Proceedings*, 10, 2031-2050.

1012 James R.H., Rudnicki M.D., Palmer M.R. (1999) - The alkali element and boron geochemistry of
1013 the Escanaba Trough sediment-hosted hydrothermal system. *Earth Planet. Sci. Lett.*, 171,
1014 157-169.

1015 Jaskula B.W. (2020) - Mineral Commodities Summary. Lithium data sheet. USGS, Report 703,
1016 648-4908.

1017 Kesler S.E., Gruber P.W., Medina P.A., Keoleian G.A., Everson M.P., Wallington T.J. (2012) -
1018 Global lithium resources: Relative importance of pegmatite, brine and other deposits. *Ore*
1019 *Geology Reviews,* 48, 55-69.

1020 Kharaka Y.K., Lico M.S. and Law L.M. (1982) - Chemical geothermometers applied to formation
1021 waters, Gulf of Mexico and California Basins (abstract). *A.A.P.G. Bull.*, 66, 588.

1022 Kharaka Y.K., Mariner R.H. (1989) - Chemical geothermometers and their application to
1023 formation waters from sedimentary basins. *In: Naeser N.D. and McCulloch T.H. (Eds),*
1024 *Thermal History of Sedimentary Basins: Methods and Case Histories. Springer-Verlag, New*
1025 *York*, 99-117.

1026 Kölbel L., Kölbel T., Sauter M., Schäfer T., Siefert D., Wiegand B. (2020) - Identification of
1027 fracture zones in geothermal reservoirs in sedimentary basins: A radionuclide-based
1028 approach. *Geothermics*, 85, 101764.

1029 Le Carlier C., Royer J.-J., Flores E.-L. (1994) - Convective heat transfer at Soultz-sous-Forêts
1030 geothermal site: implications for oil potential. *First Break*, 12, 553-560.

1031 Ledésert B., Joffre J., Ambles A., Sardini P., Genter A., Meunier A. (1996) - Organic matter in
1032 the Soultz HDR granitic thermal heat exchanger (France): a natural tracer of fluid circulations
1033 between the basement and its sedimentary cover. *J. Volcanol. Geotherm. Res.*, 70, 235-253.

1034 Ledésert B., Berger G., Meunier A., Genter A., Bouchet A. (1999) - Diagenetic-type reactions
1035 related to hydrothermal alteration in the Soultz-sous-Forêts granite, France. *Eur. J. Mineral.*,
1036 11, 731-741.

1037 Le Masne D., Lambert M. (1993) - Aquifères profonds d'Alsace. Constitution d'une base de
1038 données à usage géothermique. *SGN/IMRG Report 93 T37*, 32 p. + Appendixes.

1039 Li R.Q., Liu C.L., Jiao P.C., Wang J.Y. (2018a) - The tempo-spatial characteristics and forming
1040 mechanism of Lithium-rich brines in China. *China Geology*, 1, 72-83.

1041 Li J., Huang X.L., Wei G.J., Liu Y., Ma J.L., Han L., He P.L. (2018b) - Lithium isotope
1042 fractionation during magmatic differentiation and hydrothermal processes in rare-metal
1043 granites. *Geochim. Cosmochim. Acta*, 240, 64-79.

1044 Li Q., Fan Q., Wang J., Qin Z., Zhang X., Wei H., Du Y., Shan F. (2019) - Hydrochemistry,
1045 distribution and formation of lithium-rich brines in salt lakes on the Qinghai-Tibetan Plateau.
1046 *Minerals*, 9, 528, 15 p. doi:10.3390/min9090528.

1047 Lin Y. (1996) - Hydrogeochemical features of K-rich brine and its genetic significance in West
1048 Sichuan Basin. *J. Salt Lake Science*, 4 (1), 1-12 (in Chinese with English abstract).

1049 Lin Y. (2001) - Conditions for Sichuan Basin to trap Triassic Brine. *Geology of Chemical*
1050 *Minerals*, 23 (1), 22-23 (in Chinese with English abstract).

1051 Lin Y.T., He J.Q., Ye M.C. (2002) - Distribution types of characters of potassium-bearing brine
1052 resources in Sichuan Basin. *Geology of Chemical Minerals*, 24 (4), 215-247 (in Chinese with
1053 English abstract).

1054 Lin Y.T., Yao Y.C., Kang Z.H. (2004) - Study on the geochemical characteristics and resource
1055 significance of the highly-mineralized potassium-rich brine in Sichuan Xuanda Salt Basin.
1056 *Journal of Salt Lake Research*, 12 (1), 8-17 (in Chinese with English abstract).

1057 Lippmann M., Truesdell A., Frye G. (1999) - The Cerro Prieto and Salton Sea geothermal fields.
1058 Are they really alike? *Proc. 24th Workshop on Geothermal Reservoir Engineering, Stanford*
1059 *University, Stanford, California, January 25-27*, 10 p.

1060 Liu S., Li Y., Liu J., Ju Y., Liu J., Yang Z., Shi Y. (2018) - Equilibrium lithium isotope fractionation
1061 in Li-bearing minerals. *Geochim. Cosmochim. Acta*, 235, 360-375.

1062 López Steinmetz R.L., Salvi S., Garcia M.G., Beziat D., Franco G., Constantini O., Cordoba
1063 F.E., Caffe P.J. (2018) - Northern Puna Plateau-scale survey of Li brine-type deposits in the
1064 Andes of NW Argentina. *J. of Geochem. Explor*, 190 (2), 26-38. 10.1016/j.gexplo.
1065 2018.02.013.

1066 López Steinmetz RL, Salvi S. (2021) - Brine grades in Andean salars: when basin size matters.
1067 A review of the Lithium Triangle. *Earth-Science Reviews*, 217, 103615.

1068 Lo Ré C., Kaszuba J.P., Moore J.N., McPherson B.J. (2014) - Fluid-rock interactions in CO_2-
1069 saturated, granite-hosted geothermal systems: implications for natural and engineered
1070 systems from geochemical experiments and models. *Geochim. Cosmochim. Acta*, 141, 160-
1071 178.

1072 Ludwig F., Stober I., Bucher K. (2011) - Hydrochemical groundwater evolution in the Bunter
1073 sandstone sequence of the Odenwald Mountain Range, Germany: a laboratory and field
1074 study. *Aquatic Geochem.*, 17, 165-193.

1075 Martin C., Ponzevera E., Harlow G. (2015) - *In situ* lithium and boron isotope determinations in
1076 mica, pyroxene, and serpentine by LA-MC-ICP-MS. *Chem. Geol.*, 412, 107-116.

1077 Maurel P., Volfinger M. (1977) - Fixation du lithium en traces dans une phengite de synthèse.
1078 *Clay Min.*, 12, 163-169.

1079 McDowell L.L., Marshall C.E. (1962) - Ionic properties of mica surfaces. *Soil Sci. Soc. Amer.*
1080 *Proc.*, 93, 547-551.

1081 McKibben M.A., Williams A.E., Elders W.A., Eldridge C.S. (1987) - Saline brines and
1082 metallogenesis in a modern sediment-filled rift: the Salton Sea geothermal system,
1083 California, USA. *Appl. Geochem.*, 2, 563-578.

1084 Merceron Th., Inoue A., Bouchet A., Meunier A. (1987) - Donbassite et tosudite lithinifères à
1085 Echassières. *Géologie de la France*, n°2-3, 271-278.

1086 Michard G. (1985) - Équilibre entre minéraux et solutions géothermales. *Bulletin de Minéralogie*,
1087 108, 29-44.

1088 Michard G. (1990) - Behaviour of major elements and some trace elements (Li, Rb, Cs, Fe, Mn,
1089 W, F) in deep hot waters from granitic areas. *Chem. Geol.*, 89, 117-134.

1090 Michard G., Roekens E. (1983) - Modelling of the chemical composition of alkaline waters.
1091 *Geothermics*, 12, 161-169.

1092 Millot R., Scaillet B., Sanjuan B. (2010) - Lithium isotopes in island arc geothermal systems:
1093 Guadeloupe, Martinique (French West Indies) and experimental approach. *Geochim.*
1094 *Cosmochim. Acta,* 74, 1852-1871.

1095 Misra S., Froelich P.N. (2012) - Lithium isotope history of Cenozoic seawater: changes in
1096 silicate weathering and reverse weathering. *Science*, 335, 818-823.

1097 Moeck I.S. (2014) - Catalog of geothermal play types based on geological controls. *Renewable*
1098 *and Sustainable Energy Reviews*, 867-882.

1099 Moldovanyi E.P., Walter L.M., Land L.S. (1993) - Strontium, boron, oxygen, and hydrogen
1100 isotope geochemistry of brines from basal strata of the Gulf Coast sedimentary basin, USA.
1101 *Geochim. Cosmochim. Acta*, 57, 2083-2099.

1102 Mosser Ch., Gall J.-C., Tardy Y. (1971) - Géochimie des illites du grès à Voltzia du
1103 Buntsandstein Supérieur des Vosges du Nord, France. *Chem. Geol.*, 157-177.

1104 Munk L.A., Boutt D.F., Hynek S.A., Moran B.J. (2018) - Hydrogeochemical fluxes and processes
1105 contributing to the formation of lithium-enriched brines in a hyper-arid continental basin.
1106 *Chem. Geol.*, 493, 37-57.

1107 Nicholson K. (1993) - Geothermal fluids. Chemistry and Exploration Techniques. *Springer-*
1108 *Verlag Berlin, Heidelberg*, 260 p.

1109 Ogorodova L.P., Kiseleva I.A., Melchakova L.V. (2010) - Thermodynamic properties of lithium
1110 micas. *ISSN 0016 7029, Geochemistry International*, 48, 4, 415-418. *© Pleiades Publishing,*
1111 *Ltd., 2010. Original Russian Text © L.P. Ogorodova, I.A. Kiseleva, L.V. Melchakova, 2010,*
1112 *published in Geokhimiya*, 2010, 48, 4, 442-445.

1113 Pauwels H., Lambert M., Genter A. (1991) - Valorisation des fluides géothermaux contenant du
1114 lithium en vue d'une production industrielle. *Rapport BRGM-IMRG R 33547*, 173 p +
1115 annexes.

1116 Pauwels H., Fouillac C., Fouillac A.M. (1993) - Chemistry and isotopes of deep geothermal
1117 saline fluids in the Upper Rhine Graben: Origin of compounds and water-rock interactions.
1118 *Geochim. Cosmochim. Acta*, 57, 2737-2749.

1119 Radilla G., Sausse J., Sanjuan B., Fourar M. (2012) - Interpreting tracer tests in the enhanced
1120 geothermal system (EGS) of Soultz-sous-Forêts using the equivalent stratified medium
1121 approach. *Geothermics,* 44, 43-51.

1122 Reed M.H. (1982) - Calculation of multicomponent chemical equilibria and reaction processes in
1123 systems involving minerals, gases, and an aqueous phase. *Geochim. Cosmochim. Acta*, 46,
1124 513-528.

1125 Reed M.H., Spycher N.F. (1984) - Calculation of pH and mineral equilibria in hydrothermal
1126 waters with application to geothermometry and studies of boiling and dilution. *Geochim.*
1127 *Cosmochim. Acta*, 48, 1479-1492.

1128 Regenspurg S., Wiersberg Th., Brandt W., Huenges E., Saadat A., Schmidt K., Zimmermann G.
1129 (2010) - Geochemical properties of saline geothermal fluids from the in-situ geothermal
1130 laboratory Groß Schönebeck (Germany). *Chemie der Erde, 70*, S3, 3-12.

1131 Regenspurg S., Feldbuscha E., Byrne J., Deon F., Driba D. L., Henninges J., Kappler A.,
1132 Naumann R., Reinsch Th., Schubert Ch. (2015) - Mineral precipitation during production of
1133 geothermal fluid from a Permian Rotliegend reservoir. *Geothermics*, 54, 122-135.

1134 Riley J.P., Tongudai M. (1964) - The lithium content of sea water. *Deep Sea Research and*
1135 *Oceanographic Abstracts*. 11 (4), 563-568. https://urldefense.com/v3/https://doi.org/10.1016/
1136 0011-7471(64)90002-6;!!KbSiYrE!xLsn_fcag2DVFspXdbQP-zEruzgKeGoLmWMskuxNSCoz
1137 Mgehaobap2aH6LD8EG0N$.

1138 Risacher F. (1984) - Origine des concentrations extrêmes en bore et en lithium dans les
1139 saumures de l'Altiplano bolivien. *C. R. Académie des Sciences de Paris, t. 299, série II*, n°11,
1140 701-706.

1141 Risacher F., Fritz B. (2000) - Bromine geochemistry of salar de Uyuni and deeper salt crusts,
1142 Central Altiplano, Bolivia. *Chem. Geol.*, 176, 373-392.

1143 Risacher F., Alonso H., Salazar C. (2003) - The origin of brines and salts in Chilean Salars: a

1144 hydrochemical review. *Earth-Science Reviews*, 63, 249-292.

1145 Rittenhouse G. (1967) - Bromine in oil field waters and its use in determining possibilities of
1146 origin of the water. *Bull. Am. Assoc. Petrol. Geol.*, 51, 2430-2440.

1147 Rudnick R.L, Gao S. (2014) - Composition of the Continental Crust. *Treatise on Geochemistry:*
1148 *Second edition. Elsevier Inc*.

1149 Sanjuan B., Millot R. (2009) - Bibliographical review about Na/Li geothermometer and Lithium
1150 isotopes applied to worldwide geothermal waters. *BRGM/RP-57346-FR report*, 58 p.

1151 Sanjuan B., Michard G., Michard A. (1990) - Origine des substances dissoutes dans les eaux
1152 des sources thermales et des forages de la région Asal Ghoubbet (République de Djibouti).
1153 *J. Volcan. Geotherm. Res.*, 43, 333 352.

1154 Sanjuan B., Pinault J.-L., Rose P., Gérard A., Brach M., Braibant G., Crouzet C., Foucher J.-C.,
1155 Gautier A., and Touzelet S. (2006) - Tracer testing of the geothermal heat exchanger at
1156 Soultz-sous-Forêts (France) between 2000 and 2005. *Geothermics*, 35, 622-653.

1157 Sanjuan B., Millot R., Dezayes Ch., Brach M. (2010) - Main characteristics of the deep
1158 geothermal brine (5 km) at Soultz-sous-Forêts (France) determined using geochemical and
1159 tracer test data. *CR. Geoscience,* 342, 546-559.

1160 Sanjuan B., Millot R., Asmundsson R., Brach M., Giroud N. (2014) - Use of two new Na/Li
1161 geothermometric relationships for geothermal fluids in volcanic environments. *Chem. Geol.*,
1162 389, 60-81.

1163 Sanjuan B., Brach M., Genter A., Sanjuan R., Scheiber J., Touzelet S. (2015) - Tracer testing of
1164 the EGS site at Soultz-sous-Forêts (Alsace, France) between 2005 and 2013. *In: Proc. World*
1165 *Geothermal Congress 2015, Melbourne, Australia, 19-25 April 2015*, 12 p.

1166 Sanjuan B., Millot R., Innocent Ch., Dezayes Ch., Scheiber J., Brach M. (2016a) - Main
1167 geochemical characteristics of geothermal brines collected from the granite basement in the

1168 Upper Rhine Graben and constraints on their deep temperature and circulation. *Chem.*
1169 *Geol.,* 428, 27-47.

1170 Sanjuan B., Scheiber J., Gal F., Touzelet S., Genter A., Villadangos G. (2016b) - Inter-well
1171 chemical tracer testing at the Rittershoffen geothermal site (Alsace, France). *In: Proc.*
1172 *European Geothermal Congress 2016*, *Strasbourg, France, 19-24 September 2016*, 7 p.

1173 Sanjuan B., Millot R., Bosia C., Genter A. (2019) - Existing operating site referencing report with
1174 site selection for the pilot tests. *European EIT Raw Materials EuGeLi projet, D-8.1*
1175 *Deliverable*, 21 p.

1176 Sanjuan B., Gourcerol B., Millot R., Rettenmaier D., Jeandel E. (2020) - Geothermal lithium
1177 resource assessment in Europe. *European EIT Raw Materials EuGeLi projet, D-0.1*
1178 *Deliverable*, 86 p.

1179 Sanjuan B., Négrel G., Le Lous M., Poulmarch E., Gal F., Damy P.-C. (2021) - Main
1180 geochemical characteristics of the deep geothermal brine at Vendenheim (Alsace, France)
1181 with constraints on temperature and fluid circulation. *Proc. World Geothermal Congress*
1182 *2020+1, Reykjavik, Iceland, April - October 2021*, 12 p.

1183 Sanyal S.K. (2005) - Classification of the geothermal systems. A possible scheme. *Proc. 30th*
1184 *Workshop on Geothermal Reservoir Engineering, Stanford University, California, January 31*
1185 *- February 2, 2005*, 8 p.

1186 Savage D., Bateman K., Milodowski A.E., Hughes C.R. (1993) - An experimental evaluation of
1187 the reaction of granite with streamwater, seawater and NaCl solutions at 200°C. *J. Volcan.*
1188 *Geotherm. Res.*, 57, 167-191.

1189 Schmidt R.B., Bucher K., Drüppel K., Sober I. (2017) - Experimental interaction of hydrothermal
1190 Na-Cl solution with fracture surfaces of geothermal reservoir sandstone of the Upper Rhine
1191 Graben. *Applied Geochemistry*, 22 p. doi: 10.1016/j.apgeochem.2017.03.010.

1192 Schmidt N. (2019) - Genesis and distribution of lithium enriched pore brines at the salar de
1193 Uyuni, Bolivia. *Ph.D. Thesis, TU Freiberg, Freiberg, Germany*.

1194 Shannon R.D (1976) - Revised effective ionic-radii and systematic studies of interatomic
1195 distances in halides and calcogenides. *Acta Crystallogr. Sect. A32*, 751-767.

1196 Shaw D.M., Sturchio N.C. (1992) - Boron-lithium relationships in rhyolites and associated
1197 thermal waters of young silicic calderas, with comments on incompatible element behavior.
1198 *Geochim. Cosmochim. Acta*, 56, 3723-3731.

1199 Shouakar-Stash O., Alexeev S.V., Frape S.K., Alexeeva L.P., Drimmie R.J. (2007) -
1200 Geochemistry and stable isotopic signatures, including chlorine and bromine isotopes, of the
1201 deep groundwaters of the Siberian Platform, Russia. *Appl. Geochem.*, 22, 589-605.

1202 Sieland R. (2014) - Hydraulic Investigations of the salar de Uyuni, Bolivia. *Ph.D. Thesis, TU*
1203 *Freiberg, Freiberg*, Germany.

1204 Spycher N., Peiffer L., Sonnenthal E.L., Saldi G., Reed M.H., Kennedy B.M. (2014) - Integrated
1205 multicomponent solute geothermometry. *Geothermics*, 51, 113-123. DOI: DOI:10.1016/
1206 j.geothermics.2013.10.012.

1207 Stober I. (2014) - Hydrochemical properties of deep carbonate aquifers in the SW German
1208 Molasse Basin. *Geothermal Energy*, 2, 13, 20 p.

1209 Stober I., Bucher K. (1999a) - Deep groundwater in the crystalline basement of the Black Forest
1210 region. *Applied Geochemistry*, 14 (2), 237-254.

1211 Stober I., Bucher K. (1999b) - Origin of salinity of deep groundwater in crystalline rocks. *Terra*
1212 *Nova*, 11 (4), 181-185.

1213 Stueber A.M., Walter L.M., Huston T.J., Pushkar P. (1993) - Formation waters from
1214 Mississippian-Pennsylvanian reservoirs, Illinois basin, USA: chemical and isotopic
1215 constraints on evolution and migration. *Geochim. Cosmochim. Acta*, 57, 763-784

1216 Sturchio N.C., Chan L.H. (2003) - Lithium Isotope Geochemistry of the Yellowstone
1217 Hydrothermal System. *Society of Economics Geologists*, Chapter 11, 1-10.

1218 Tabarès (2013) - Lithium Technology, Performance and Safety. *Nova Science Publishers*.

1219 Teng F.Z., McDonough W.F., Rudnick R.L., Dalpé C., Tomascak P.B., Chappell B.W., Gao S.
1220 (2004) Lithium isotopic composition and concentration of the upper continental crust.
1221 *Geochim. Cosmochim. Acta*, 68, 4167-4178.

1222 Torrente M.M., Milia A. (2013) - Volcanism and faulting of the Campania margin (Eastern
1223 Tyrrhenian Sea, Italy): A three-dimensional visualization of a new volcanic field off Campi
1224 Flegrei. Bull Volcanol, 75:719, doi 10.1007/s00445-013-0719-0.

1225 Tran T., Luong V.T. (2015) - Chapter 3: Lithium Production Processes A2 - Chagnes,
1226 Alexandre. *Lithium Process Chemistry*. J. Światowska. Amsterdam, Elsevier: 81-124.

1227 Ventura S., Bhamidi S., Hornbostel M., Nagar A., Perea E. (2016) - Selective recovery of metals
1228 from geothermal brines. *Washington, D.C., U.S. Dept. of Energy. Office of Energy Efficiency*
1229 *and Renewable Energy*.

1230 Vernoux J.-F., Lambert M. (1993) - Aquifères profonds d'Alsace. Constitution d'une base de
1231 données à usage géothermique. *Final report SGN/IRG ARG 93 T37*, 41 p.

1232 Vidal J., Patrier P., Genter A., Beaufort D., Dezayes Ch., Glaas C., Lerouge C., Sanjuan B.
1233 (2018) - Clay minerals related to the circulation of geothermal fluids in boreholes at
1234 Rittershoffen (Alsace, France). *J. Volcan. Geotherm. Res.*, 349, 192-204.

1235 Vigier N., Decarreau A., Millot R., Carignan J., Petit S., France-Lanord C. (2008) - Quantifying Li
1236 isotope fractionation during smectite formation and implications for the Li cycle. *Geochim.*
1237 *Cosmochim. Acta*, 72, 780-792.

1238 Warren E.A., Smalley P.C. (1994) - North Sea formation waters Atlas. *Geological Society*
1239 *Memoir 15, Geological Society Publishing House, Bath,* 208 p.

1240 Werner H.H. (1970) - Contribution to the mineral extraction from supersaturated geothermal
1241 brines, Salton Sea area, California. *Geothermics, Special issue, U.N. Symposium on the*
1242 *Development and Utilization of Geothermal Resources, Pisa, vol. 2, Part 2*, 1651-1655.

1243 Wheildon J., Francis M.F., Ellis J.R.L., Thomas-Betts A. (1980) - Exploration and interpretation
1244 of the S.W. England geothermal anomaly. *In: A. Strub and P. Ungemach (Editors), Proc. 2nd*
1245 *Int. Semin. on Results of EC Geothermal Energy Research, March 4-6, 1980, Strasbourg.*
1246 *Reidel, Dordrecht*, 456-465.

1247 Williams A.E., McKibben M.A. (1989) - A brine interface in the Salton Sea geothermal system,
1248 California: fluid geochemical and isotopic characteristics. *Geochim. Cosmochim. Acta*, 53,
1249 1905-1920.

1250 Williams L.B., Hervig R.L. (2005) - Lithium and boron isotopes in illite-smectite: the importance
1251 of crystal size *Geochim. Cosmochim. Acta*, 69, n°24, 5705-5716.

1252 Wilson T.P., Long D.T. (1993) - Geochemistry and isotope chemistry of Michigan Basin brines:
1253 Devonian formations. *Appl. Geochem.*, 8, 81-100.

1254 Wimmenauer W. (2003) - Erläuterungen zur Geologischen Karte 1:25 000 Blatt Kaiserstuhl.

1255 Zhang L., Chan L.H., Gieskes J.M. (1998) - Lithium isotope geochemistry of pore waters from
1256 Ocean Drilling Program Sites 918 and 919, Irminger Basin. *Geochim. Cosmochim. Acta*, 62,
1257 2437-2450.

List of captions

Figure 1 - Map of Europe showing the six main geothermal areas with Li-rich fluids (red circles) and Li-concentration ranges in such fluids. The highest Li values are found in Italy (but no geothermal well is presently usable), and in Germany and France, especially in the Upper Rhine Graben (URG) where several geothermal sites are in operation (from Sanjuan *et al.*, 2020).

Figure 2 - Location of deep fluids in the Upper Rhine Graben (URG) and stratigraphic positions of wells and reservoirs (from Sanjuan *et al.*, 2016a).

Figure 3 - Map of temperatures extrapolated at a 5 km depth (based on Hurtig *et al.*, 1992).

Figure 4 - Schematic NW-SE cross-section of the Upper Rhine Graben (from Le Carlier *et al.*, 1994, and Sanjuan *et al.*, 2010, 2016a) showing several deep wells (Bruchsal, Cronenbourg, Landau, Insheim, Soultz, Rittershoffen, Vendenheim, Illkirch, etc.) drilled to depths of 2540 to 5000 m. Thermal-gradient values of 40 to 60 °C/km were observed in the URG sedimentary formations of deep wells (Vernoux and Lambert, 1993). Based on geochemical and geothermometric arguments, Sanjuan *et al.* (2016a) suggest that the Triassic Buntsandstein sandstone at depths of ≥ 4 km (in the graben centre) could represent the potential reservoir at 225 ± 25°C for most of the these brines. The deep geothermal brine would then migrate from the graben centre to its outer boundaries, circulating both in granite and in the deep sedimentary rocks through a complex system of deep, still poorly defined faults (probably NW-SE, but also NE-SW).

Figure 5 - Concentrations of Cl *versus* Na with Li-concentration ranges for deep fluids in the BRGM-EIFER database.

Figure 6 - Log K *versus* Log Na (mg/l) for the Li-rich fluids, integrating the isotherms calculated with the Na-K thermometric relationships of Fournier (1979) and Giggenbach (1988). The well-known Salton Sea geothermal area in California (USA), with high-temperature (330-360 °C) and high-TDS brines, indicating high Li concentrations (see Table 1; Werner, 1970; Elders and Cohen, 1983; Mc Kibben *et al.*, 1987; Williams *et al.*, 1989; Lippmann *et al.*, 1999; Birkle *et al.*, 2010; Mazzini *et al.*, 2011) was integrated here as volcanic reference area.

Figure 7 - Main different Na-Li thermometric relationships found in the literature, presented as a diagram Log (Na/Li) *versus* 1000/T (Na/Li ratio is calculated in mol/l).

Figure 8 - Log Li *versus* Log Na (mg/l) for Li-rich fluids, integrating the isotherms calculated using the Na-Li thermometric relationships determined by Fouillac and Michard (1981) for Cl ≥ 0.3 M, and by Kharaka *et al.* (1982) and Sanjuan *et al.* (2014) (see Figure 6).

Figure 9 - Log (Na/Li) *versus* Log (Na/K), with molar ratios, for deep Li-rich fluids of this study, integrating the Na-K (Fournier, 1979; Gigenbach, 1988) and Na-Li (Fouillac and Michard, 1981; Kharaka *et al.*, 1982; Sanjuan *et al.*, 2014) thermometric relationships.

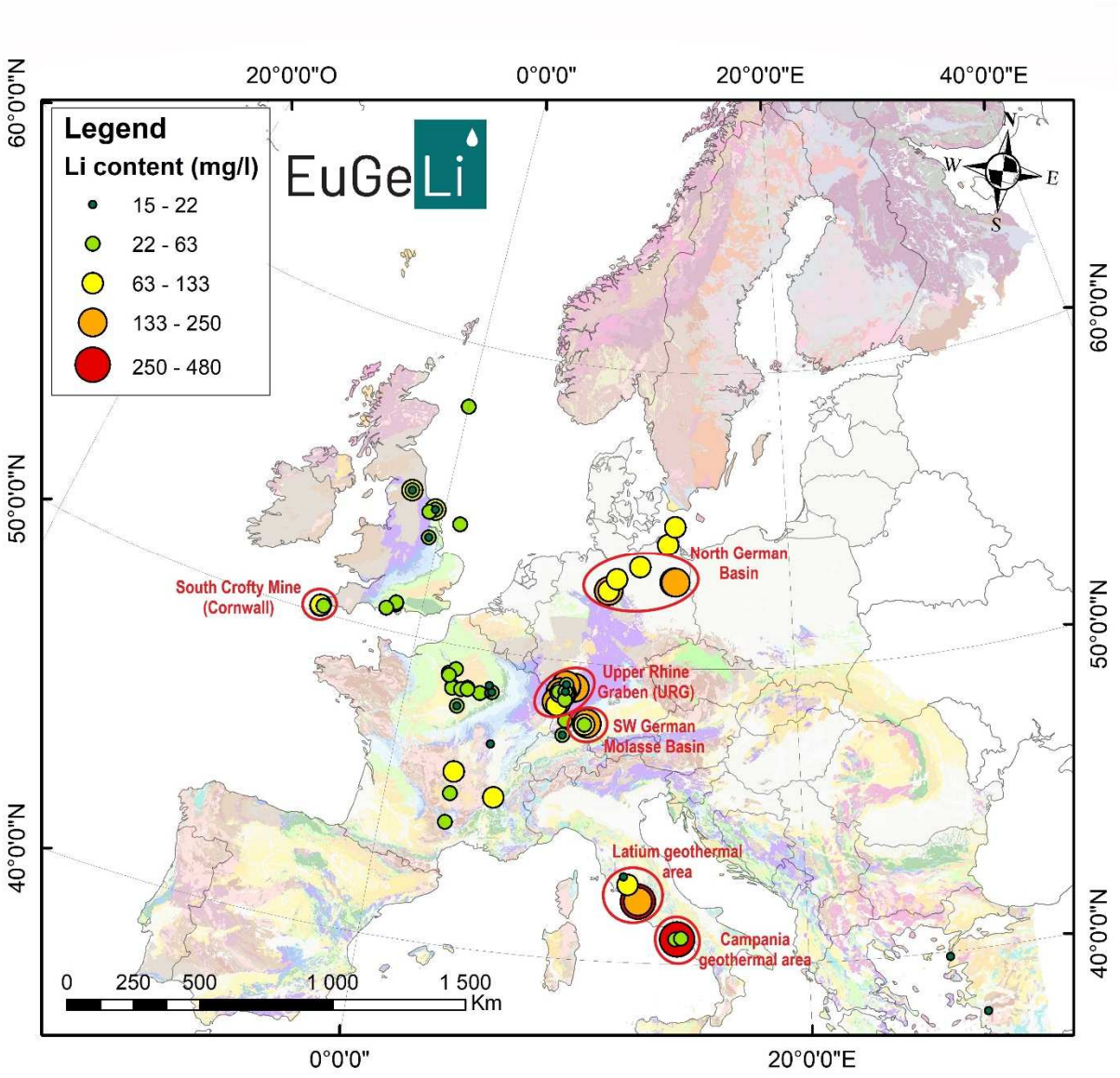
Legend
Li content (mg/l)
15 - 22
22 - 63
63 - 133
133 - 250
250 - 480
EuGeLi
20°0'0"O
0°0'0"
20°0'0"E
40°0'0"E
60°0'0"N
50°0'0"N
40°0'0"N
N
W
E
S
North German Basin
South Crofty Mine (Cornwall)
Upper Rhine Graben (URG)
SW German Molasse Basin
Latium geothermal area
Campania geothermal area
0 250 500 1 000 1 500
Km

Figure 1

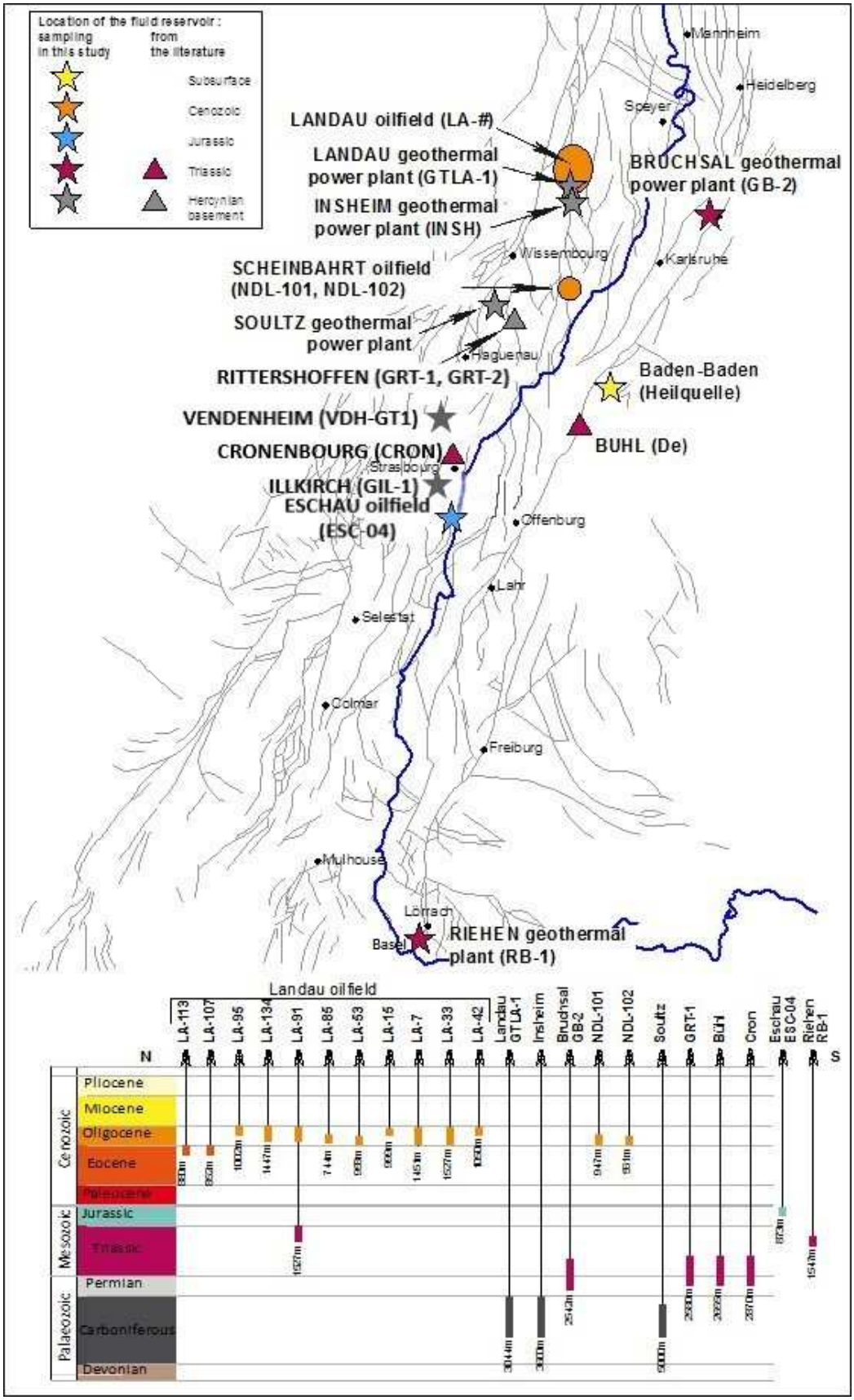
Location of the fluid reservoir :
sampling in this study
from the literature
Subsurface
Cenozoic
Jurassic
Triassic
Hercynian basement
LANDAU oilfield (LA-#)
LANDAU geothermal power plant (GTLA-1)
INSHEIM geothermal power plant (INSH)
SCHEINBAHRT oilfield (NDL-101, NDL-102)
SOULTZ geothermal power plant
RITTERSHOFFEN (GRT-1, GRT-2)
VENDENHEIM (VDH-GT1)
CRONENBOURG (CRON)
ILLKIRCH (GIL-1)
ESCHAU oilfield (ESC-04)
BRUCHSAL geothermal power plant (GB-2)
Baden-Baden (Heilquelle)
BUHL (De)
RIEHEN geothermal plant (RB-1)
Mannheim
Heidelberg
Speyer
Wissembourg
Karlsruhe
Haguenau
Strasbourg
Offenburg
Lahr
Selestat
Colmar
Freiburg
Mulhouse
Lörrach
Basel
Landau oilfield
N
S
LA-113
LA-107
LA-95
LA-134
LA-91
LA-85
LA-53
LA-15
LA-7
LA-33
LA-42
Landau GTLA-1
Insheim
Bruchsal GB2
NDL-101
NDL-102
Soultz
GRT-1
BUH
Cron
Eschau ESC-04
Riehen RB-1
Cenozoic
Mesozoic
Palaeozoic
Pliocene
Miocene
Oligocene
Eocene
Paleocene
Jurassic
Triassic
Permian
Carboniferous
Devonian

Figure 2

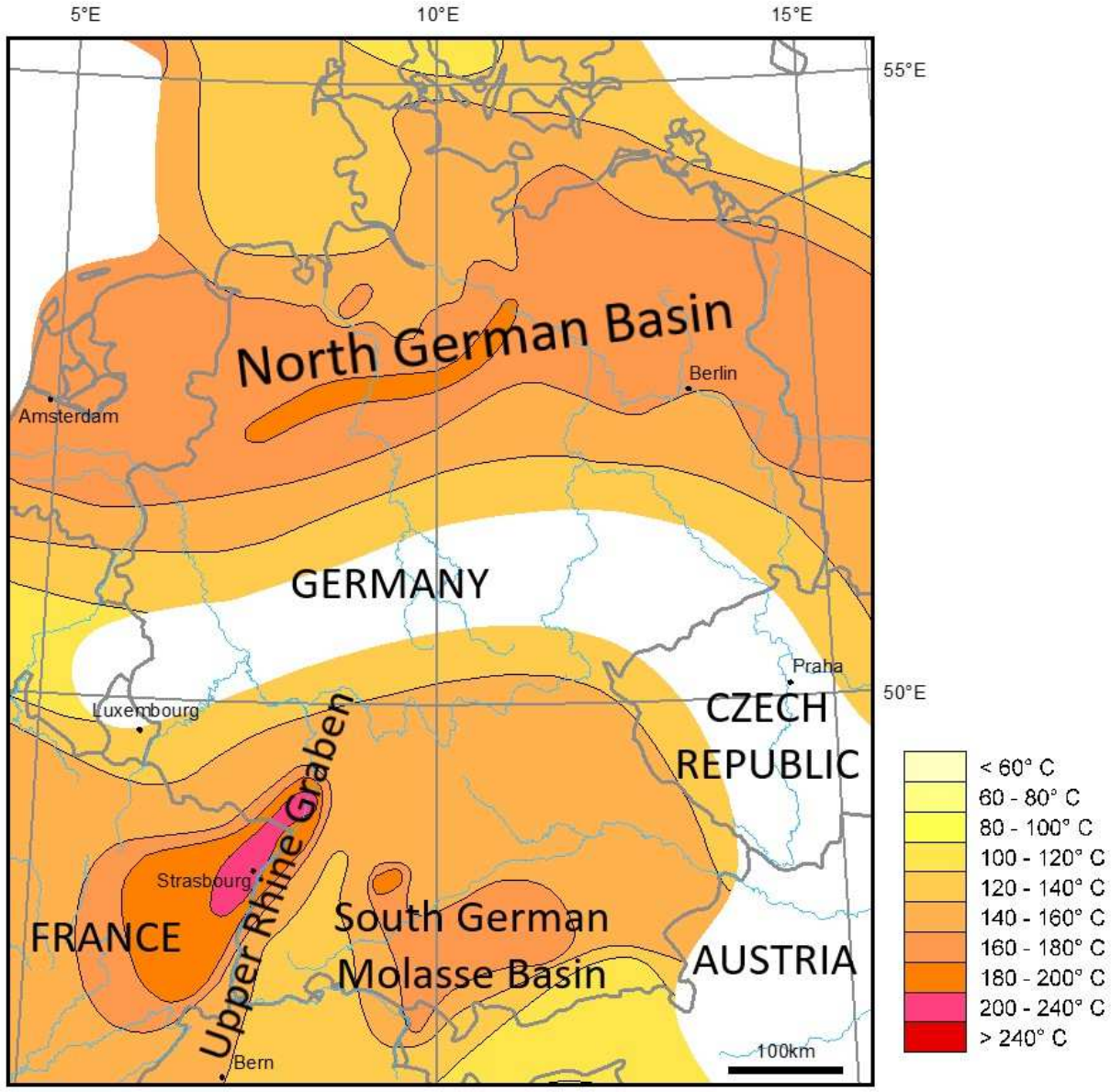
5°E
10°E
15°E
55°E
50°E
North German Basin
Berlin
Amsterdam
GERMANY
Praha
Luxembourg
CZECH
REPUBLIC
Upper Rhine Graben
Strasbourg
FRANCE
South German
Molasse Basin
AUSTRIA
Bern
100km
< 60° C
60 - 80° C
80 - 100° C
100 - 120° C
120 - 140° C
140 - 160° C
160 - 180° C
180 - 200° C
200 - 240° C
> 240° C

Figure 3

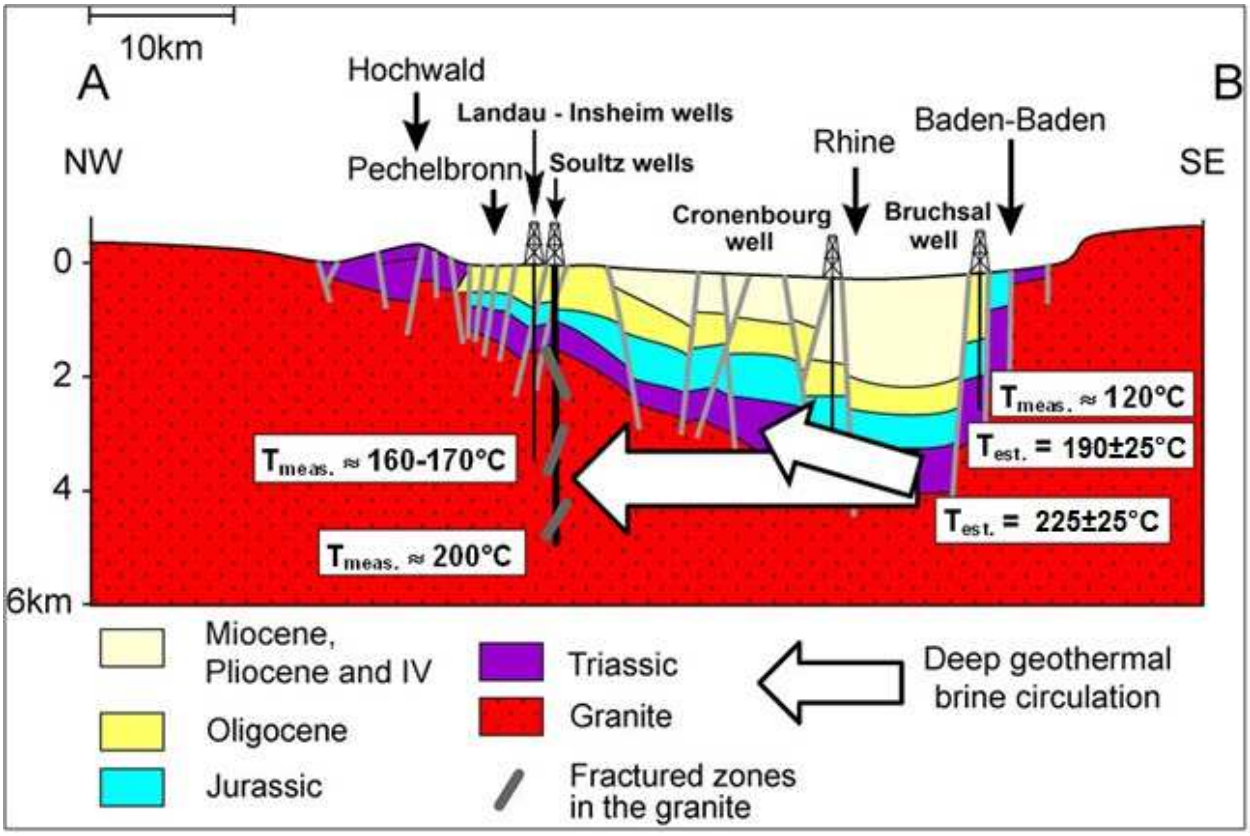

Figure 4

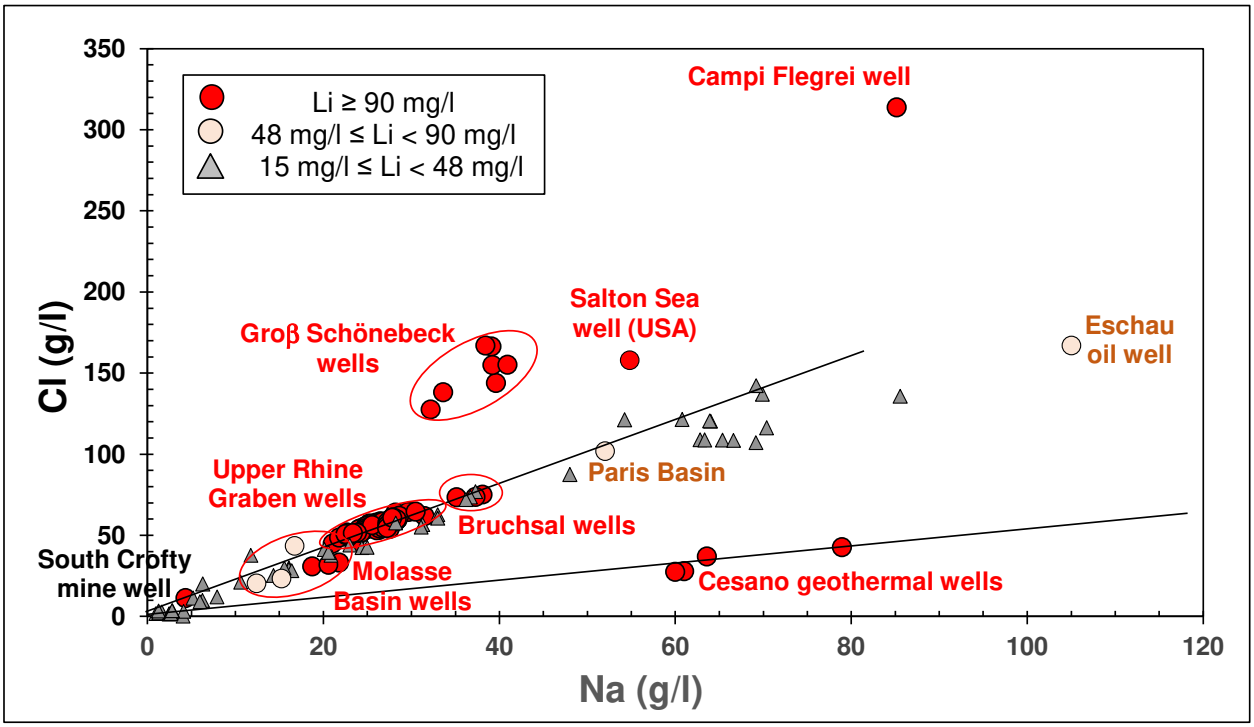

Figure 5

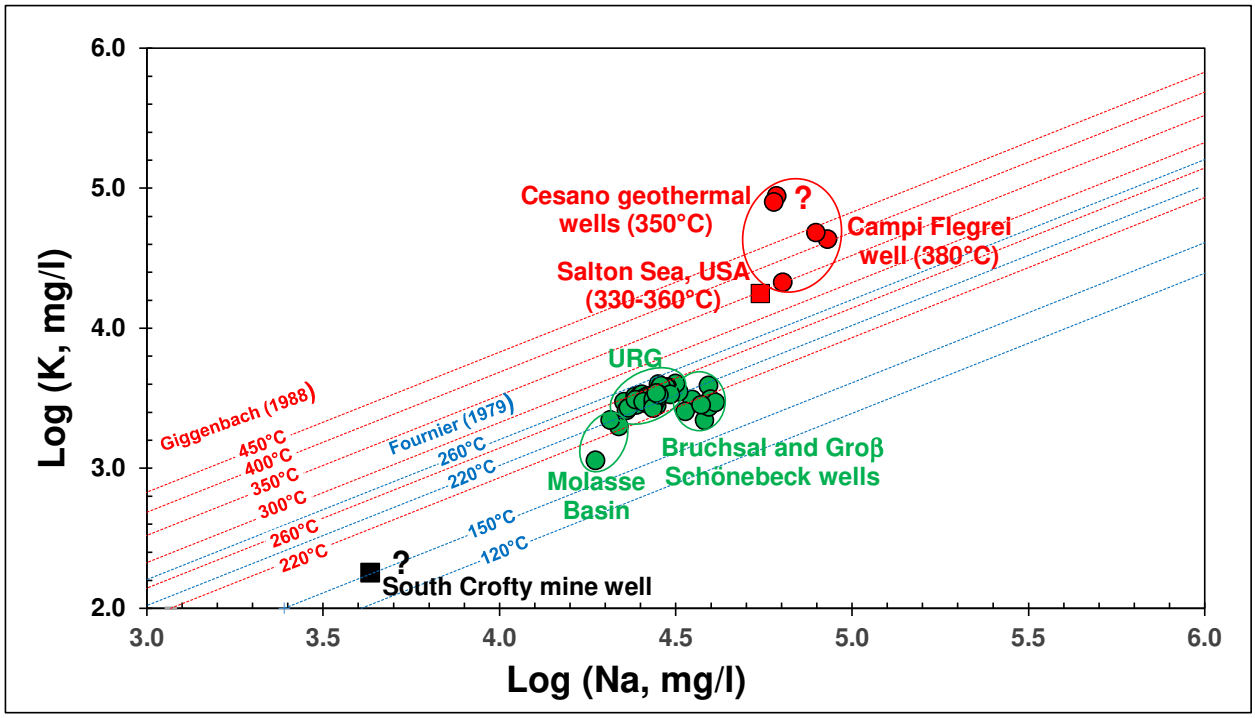

Figure 6

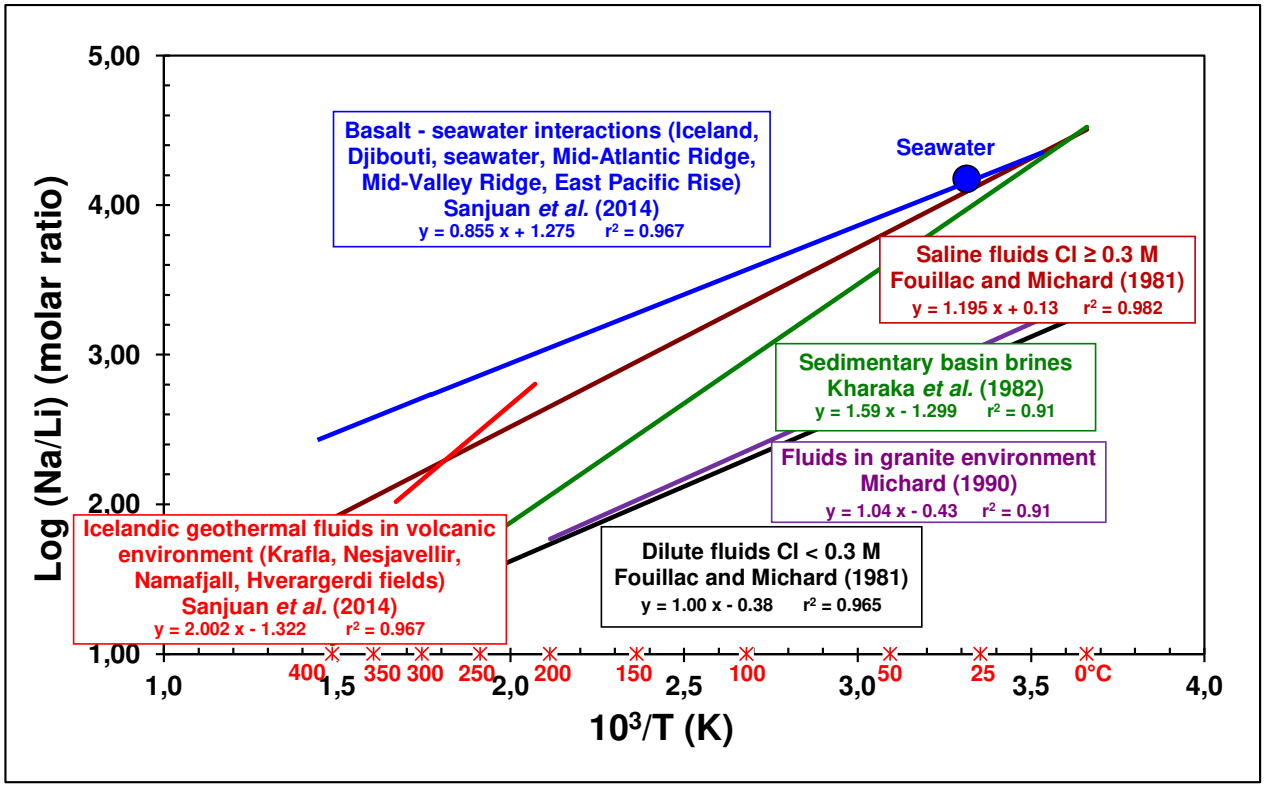

Figure 7

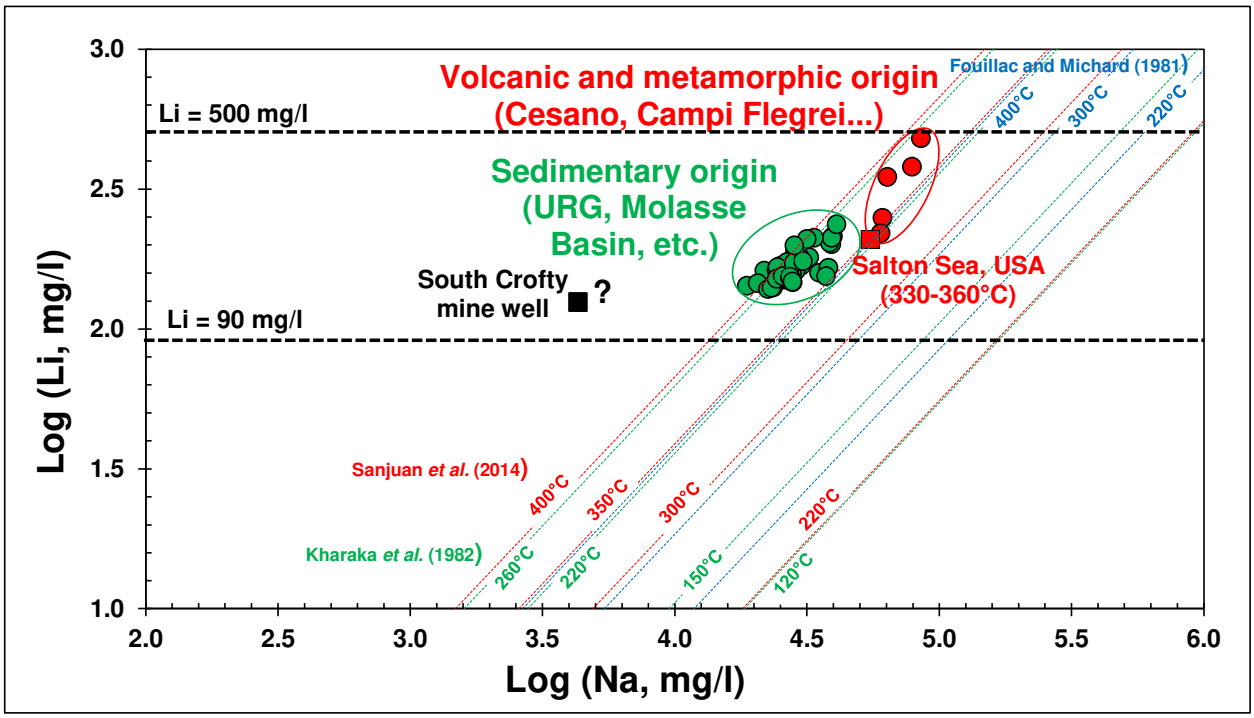

Figure 8

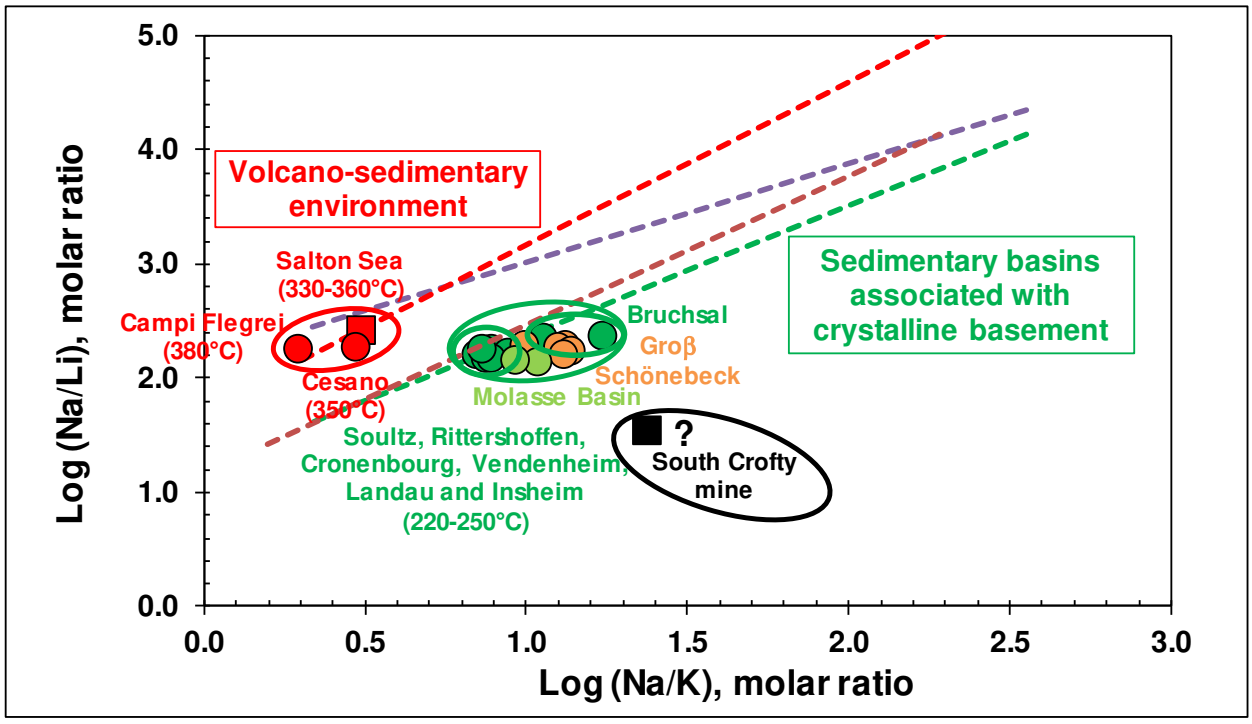

Na-Li geothermometer (Sanjuan *et al.*, 2014) - Na-K geothermometer (Giggenbach, 1988)

Na-Li (Fouillac & Michard, 1981) - Na-K (Giggenbach, 1988)

Na-Li (Kharaka *et al.*, 1982) - Na-K (Giggenbach, 1988)

Na-Li (Kharaka *et al.*, 1982) - Na-K (Fournier, 1979)

Figure 9

List of tables

Table 1 - Main geothermal and geological characteristics of the six most potential European geothermal areas with deep Li-rich fluids (Li ≥ 125 mg/l).

Geothermal system	Geological environment	Location	Reservoir rocks	Depth m	$T_{meas.\ res.}$ °C	$T_{est.\ res.}$ °C	TDS fluid g/l	Li mg/l	References
Ultra-high temperature (> 300°C) geothermal system	Sedimentary reservoirs associated with relatively young volcanic environments	Campi Flegrei geothermal area (Mofete, Italy)	Volcano-Sedimentary Complex (VSC) with Mesozoic sediments Thermo-metamorphic zone Recent volcanism developed during the Late Pliocene to Recent	2310-2699	350-380	380	516	**480**	Pauwels *et al.* (1991) Buonasorte *et al.* (1993)
		Cesano geothermal area (Italy)	Sedimentary Tuscan and Umbrian series (Upper Triassic, Mesozoic carbonate rocks). Strong thermo-metasomatic phenomena. Quaternary alkaline-potassic volcanic center of Sabatini Mt. area	960-3219	150-368	350	230-390	**220-380**	Pauwels *et al.* (1991) Buonasorte *et al.* (1993)
		Salton Sea geothermal area - Imperial Valley (Southern California, USA)	Hydrothermally altered Cenozoic-Quaternary terrigeneous deltaic sequence of sandstones with clay or carbonate cements, interbedded with lacustrine mudstones, siltstones and shales in various proportions. Quaternary (Pleistocene to Holocene) volcanic environment	2500	330-340	340-360	260-265	**200-215**	Williams and McKibben (1989) Elders and Cohen (1983)
Low to medium temperature (120-250°C) geothermal system	Tectonic sedimentary basins over a crystalline basement without an associated magmatic heat source	Groß Schönebeck geothermal area in the North German Basin (passive-active rift basin, sub-basin of the Southern Permian Basin, that accounts for a composite of intracontinental rift composed of 10-12 km of Permian to Cenozoic sediments)	Sandstones and volcanic rocks (Rotliegend, Lower Permian) Large amounts of dissolved gases (80 vol.% N_2, 15 vol.% CH_4, 5 vol.% CO_2, H_2, He…)	3500-4309	150	220	212-269	**180-237**	Regenspurg *et al.* (2010) Regenspurg *et al.* (2015)
		German Molasse Basin (South West Germany) : foreland basin of the Alps that formed during the Oligocene and Miocene because of the flexure of the European plate under the weight of the orogenic wedge of the Alps. The basin filled with a sedimentary sequence of the most part removed from the developing mountain chain by erosion and denudation	Fractured and karstified limestone/dolomite aquifer (Upper Muschelkalk)	1914-1976	67-94	210	55-62	**143-162**	Stober (2014)
		Upper Rhine Graben (URG): as a part of the European Cenozoic Rift System, it developed from c. 47 Ma onwards in response to changing lithospheric stresses in the north-western foreland of the Alps. The overlying sedimentary sequences consist of Cenozoic evaporites and claystone underlain by Mesozoic limestone and sandstone. Its basement is mainly constitued of granite							
		Bruchsal geothermal area - URG (Germany)	Triassic Buntsandstein continental red sandstone that is fined to coarse-grained with some conglomeratic beds (up to 450 m thick)	2542	120	190	121	**159**	Sanjuan *et al.* (2016a)
		Cronenbourg geothermal area - URG (France)		2870	140	200-250	104	**210**	Pauwel *et al.* (1993)
		Soultz-sous-Forêts, Rittershoffen, Vendenheim, Illkirch, Landau, Insheim geothermal areas - URG (France and Germany)	Granite basement (Carboniferous)	2580-5000	156-200	200-250	93-107	**161-190**	Sanjuan *et al.* (2016a) Sanjuan *et al.* (2021) Bosia *et al.* (2021)
Very low temperature (< 100°C) geothermal system	Cornubian batholith intruded about 290 Ma ago into Devonian argillaceous sedimentary rocks	South Crofty mine well (Cornwall, England)	Carmmenellis Granite	690	52	50-70	19	**125**	Edmunds *et al.* (1985)

Table 2 - Chemical and isotope compositions of the main deep Li-rich fluids (Li ≥ 125 mg/l) from the six most potential European geothermal areas.

Location	Well	Depth m	Fluid sampling date	pH	Na g/l	K g/l	Ca g/l	Mg mg/l	Cl g/l	SO_4 mg/l	Alk. meq/l	SiO_2 mg/l	Li mg/l	Sr mg/l	F mg/l	Br mg/l	B mg/l	$\delta^{18}O$ ‰	δD ‰	δ^7Li ‰	$^{87}Sr/^{86}Sr$	References
Campi Flegrei geothermal well (Mofete, Italy)	n°5	2310-2699	1983		85.2	43.4	54.0		314	traces	traces	210	480				231					Pauwels *et al.* (1991) Buonasorte *et al.* (1993)
Cesano geothermal well (Italy)	C-1-1 - initial	960-3219	1975	8.5	63.6	21.4	0.043	12	37.0	91010	31.2	130	350		100		2448					Pauwels *et al.* (1991)
	C-1-2 - initial	960-3219	1975	8.5	78.9	48.4	0.106	17	42.9	163290	95.9	132	380				2690					Buonasorte *et al.* (1993)
	C-1-3 - stabilized	960-3219	1982	7.9	61.0	88.0	0.070	12	28.0	191000	202	100	250		140		1508					
	C-1-4 - stabilized	960-3219	1980	7.9	60.0	80.0	0.200	20	27.5	186000	41.0	120	220				1331					
Salton Sea geothermal well	SSSDP 2-14	2500	1986	5.1	54.8	17.7	28.5	49	158	53		> 588	209	421		111	271	0.6	-73.0			Williams and McKibben (1989)
(Southern California, USA)	IID - 1	2500	1968	5.2	50.4	17.5	28.0		155	5.4		400	215									Elders and Cohen (1983)
Groß Schönebeck geothermal	GRSK-3 (injection)	4309	January 2001	5.5-6.4	39.1	3.91	56.1	437	167	139	0.50		201	1928								Regenspurg *et al.* (2010)
well (North German Basin)	GRSK-4 (production)	4400	October 2007	5.5-6.4	32.2	3.52	48.1	243	128	38			180	1139								
	GRSK-4 (4200 m)	4200	October 2007	6.8	38.4	2.90	54.0	430	167	140		79	204	1900								
	GRSK-4 (3500 m)	3500	May 2013	7.6	39.6	3.12	53.8	382	144	175		6.2	215	1570			132					Regenspurg *et al.* (2015)
	GRSK-4 (4120 m)	4120	May 2013	7.7	39.2	2.74	54.0	397	155			6.5	212	1650			142					
	GRSK-4 (4200 m)	4200	January 2014	6.3	40.9	2.96	51.2	364	155	81		90	237	1630			147					
	GRSK-4 (4240 m)	4240	January 2014	7.1	33.6	2.56	45.4	233	138	94		94	212	1290			116					
Molasse Basin well	HC-14	1914	1975-2005	6.8	18.7	1.14	0.88	351	30.8	1852	19.0		143									Stober (2014)
(South West Germany)	HC-15	1938	1975-2005	6.5	21.8	1.99	0.79	115	33.3	2065	21.6		162									
	HC-19	1976	1975-2005	6.4	20.6	2.22	1.08	195	31.9	1280	18.1		146									
Bruchsal geothermal well - Upper Rhine Graben (Germany)	GBRU-1	2542	03/04/2012	5.1	35.1	3.11	7.36	301	73.6	267	6.18	77	159	391	0.85	203	39.4	-2.8	-39.9	1.7	0.715028	Sanjuan *et al.* (2016a)
Landau geothermal well - Upper Rhine Graben (Germany)	GTLA-1	3044	20/06/2013	5.1	28.2	4.00	7.70	80	64.5	130	2.36	159	182	430	3.2	219	39.0	-1.4	-43.4	1.0	0.711512	
Insheim geothermal well - Upper Rhine Graben (Germany)	INSH	3600	20/06/2013	5.2	29.9	3.82	7.25	99	64.9	131	2.46	167	168	456	2.9	185	41.1	-1.2	-44.4	1.4	0.711513	
Cronenbourg geothermal well - Upper Rhine Graben (France)	CRON	2870	1980	6.7	31.5	4.03	4.81	126	62.0	480	2.20	143	210	405	5.5	361	37.9	-2.2	-40.0		0.711800	Sanjuan *et al.* (2016a)
Soultz-sous-Forêt geothermal well - Upper Rhine Graben (France)	GPK-2	5000	19/06/2013	5.0	28.1	3.19	7.23	131	58.6	157	2.45	201	173	455	2.9	216	40.8	-2.4	-44.0	1.4	0.711319	
Rittershoffen geothermal well - Upper Rhine Graben (France)	GRT-1	2580	10/01/2013	6.3	28.5	3.79	7.20	138	59.9	220	3.06	146	190	498	1.8	251	45.9	-2.3	-41.2	1.1	0.711466	
Rittershoffen geothermal well - Upper Rhine Graben (France)	GRT-2	3196	23/04/2018	4.9	28.4	3.59	7.47	115	59.6	97	2.34	182	161	396	1.8		37.2					BRGM Internal analysis report (2018)
Vendenheim geothermal well - Upper Rhine Graben (France)	VDH-GT1	4660	08/03/2018	7.4	28.6	3.88	3.63	66	62.0		9.52	138	162	202		261	38.6	-1.9	-39.6	2.5	0.711735	Sanjuan *et al.* (2021)
Illkirch geothermal well - Upper Rhine Graben (France)	GIL-1	3319	19/05/2019		27.2		4.08	191	54.5	400		88	173	224		320	33.0					Bosia *et al.* (2021)
South Crofty mine well (Cornwall, England)	SCMW	690	1982	6.5	4.30	0.18	2.47	73	11.5	145	1.11	34	125	40	2.7	43	11.0	-5.2	-29.0			Edmunds *et al.* (1985)